ASSOCIATION OF PUNJAB GEOGRAPHERS
1999
STRIVE TO EXCEL

punjab geographer

INSTITUTE FOR SPATIAL PLANNING & ENVIRONMENT RESEARCH
PANCHKULA

A DOUBLE BLIND PEER REVIEWED JOURNAL OF APG AND ISPER INDIA INDEXED IN SCOPUS

VOLUME 17 ISSN- 0973–3485 OCTOBER 2021

MODELING MAGNITUDE AND FREQUENCY OF FLOODS IN THE UPPER YAMUNA RIVER BASIN, INDIA

Sachin Pandwar
Omvir Singh

Abstract

Globally, floods are one of the most common hydrological disasters, but their happening to a larger extent is unpredictable. This study, therefore, aims to model the return periods and occurrence probabilities of peak flood discharges in the upper reaches of Yamuna river basin. The study is based on annual peak flood discharge series data (Q_{max}) available for nine gauge and discharge sites located in the upper Yamuna river basin. Two most commonly used probability distribution models namely Gumbel Extreme Value-I (GEV-I) and Log-Pearson Type-III (LP-III) have been used to estimate peak flood discharges in future. Likewise, two goodness-of-fit (GoF) tests, namely, Kolmogorov-Smirnov (KS) and Anderson-Darling (AD) have been applied to the fitted distributions to identify the best-fit model. The analysis of Q_{max} series has shown high inter-annual variability, as the C_v ranges between 0.47 (47 per cent) and 1.04 (104.37 per cent). The ratio of observed Q_{max} and mean annul flood (Q_m) indicates that the highest ever recorded flood is about two-to-four times larger than Q_m. Hathini Kund gauge and discharge site has recorded the largest ever peak flood discharges of 23,448, 22,837, 21,082 and 20,083 m^3/s in the years 2019, 2013, 2010 and 1978, respectively. The probability distribution used for the estimation of return periods with the magnitude of estimated discharge shows that the exceedance probability decreases with increasing time. The positive relationship between observed Q_{max} and the estimated discharge for different return periods suggests that both GEV-I and LP-III distribution models can be considered satisfactory for flood modeling. However, two goodness-of-fit tests results reveal that LP-III is more robust than GEV-I distribution model for flood modeling in the upper Yamuna river basin. The study may be useful for water resource managers in designing hydraulic structures for the management of floods in future.

Keywords: Gumbel extreme value-I, Log-Pearson type-III, Goodness-of-fit tests, Peak flood, Return period.

Introduction

Floods are one of the most recurring and destructive hydrological disasters causing immense loss of human lives and devastations of economy and environment. Floods are caused by heavy rainfall events, cloud bursts, cyclones, dam failure, storm surge and tsunamis (Singh and Kumar, 2013). Heavy rainfall events have devastating impacts on population and economic development (Trenberth et al., 2003; Ingram, 2016; Tanoue et al., 2016; Tabari, 2020). Globally, more than one-third of the total land area is prone to floods affecting about 82 per cent of the population in 90 countries. Annually, floods have been affecting about 520 million people worldwide (Adhikari et al., 2010).

Out of the total flood events in the world during the past 30 years, 40 per cent have occurred in the continent of Asia. Interestingly, flood events across Asia have increased by six-folds between 2000 and 2009, in comparison to the flood events occurred in 1970s and in 1980s, respectively. The regional distribution of floods over the continent shows that South Asia is the most affected region (Shrestha, 2008). Sharma (2012) has detected an increasing trend in the number of people affected by floods in South Asia.

Floods occur quite frequently in India. About 40 million hectares of land, roughly one-eighth of the country's geographical area is prone to floods, of which about 8 million hectares of land is affected by floods every year (Gupta et al., 2003; Mohapatra and Singh, 2003; Roy et al., 2008; Ray et al., 2019). A total of 2,443 flood events in India have caused nearly 44,991 deaths from 1978 to 2006 with an average of 1,551 deaths every year, which accounts for about one-fifth of the global death count due to floods (Singh and Kumar, 2013). Similarly, an increase in frequency, duration, severity and intensity of flood disasters has been observed over large parts of India, especially during the monsoon season (Goswami et al., 2006; Singh and Singh, 2011; Menon et al., 2013; Karuna et al., 2016; Roxy et al., 2017). Warming trends over the Indian Ocean has possibly increased moisture amount, thereby resulting in an increase in rainfall extremes over India and subsequently the floods (Rao et al., 2012; Roxy et al., 2015).

In the light of above, reliable estimates of flood magnitude and frequency are essential for flood plain management, protection of infrastructure and control of epidemics (Renard et al., 2013; Benameur et al., 2017). In the field of hydrology, probabilistic approach has been used widely to estimate the magnitude and frequency of extreme events such as floods for mitigating their devastating impacts (Helsel and Hirsch, 2010; Renard et al., 2013; Benameur et al., 2017). Selection of an appropriate probability distribution and associated parameter estimation procedure is of prime importance at site flood frequency analysis (Rahman et al., 2013). Several probabilistic models such as Generalized Extreme Value, Gumbel Extreme Value-I (GEV-I), Pearson, Log-Pearson Type-III (LP-III), Normal, Log-Normal etc. have been commonly used to estimate flood extremes (Gumbel, 1958; Chow et al., 1988; Haktanir, 1991; Haktan, 1992; Hosking and Wallis, 1993; Abdul-Karim and Chowdhury, 1995; Pandey and Nguyen, 1999; Ibrahim and Isiguzo, 2009; Ewemooje and Ewemooje, 2011; Izinyon et al., 2011; Kamal et al., 2017; Farooq et al., 2018). Within these probabilistic models, GEV-I and LP-III are the two most widely used distribution methods which have provided reliable results with respect to past characteristics of the magnitude and frequency of floods for the Indian rivers (Hire, 2000; Kumar et al., 2003; Jha and Bairagya, 2011; Mishra et al., 2013; Hire and Patil, 2018; Pandey et al., 2018; Bhat et al., 2019b; Kumar, 2019; Pawar and Hire, 2019; Pawar et al., 2020).

High magnitude floods are an integral part of the hydrologic systems of all the monsoon-fed Indian rivers. The Yamuna river, a major tributary of the Ganga River system, experiences moderate to severe floods almost every year during monsoon season. Recently, the Yamuna river basin has experienced floods in the years 1900, 1914, 1924, 1933, 1947, 1955, 1956, 1967, 1971, 1975, 1976, 1978, 1988, 1995, 1998, 2008, 2010, 2013 and 2019 (Kumar et al., 2020). The occurrence of these floods has resulted in massive loss to agriculture, human lives as well as public and private properties. In the light of these facts, the estimation of frequency, magnitude and return period of peak flood discharges can be extremely helpful in reducing the impact of floods in future. Although, a few studies on the hydrologic characteristics of rivers in the upper reaches of the Indian Himalayan region have been carried out, yet no study has been attempted on the upper reaches of Yamuna river basin. To fill this gap, an attempt has been made, in this study, to estimate the frequency, magnitude and recurrence interval of peak flood discharges in the upper reaches of Yamuna river basin.

Objectives

Major objectives of the study are:

- to analyze the spatial and temporal changes in the magnitude and frequency of floods along with causative factors of floods and
- to estimate the probability of peak flood magnitude and frequency for different return periods in the upper reaches of Yamuna river basin.

Study Area

The upper Yamuna river basin extends between 30º 14' and 31º 25' north latitudes and 77º 03' and 78º 37' east longitudes (Fig.1). It is a part of the Ganga basin and is situated in the north-western Himalayan reach. The altitude of the basin varies from 341 m to 6284 m above mean sea level. The upper parts of the basin have high mountains, most of which have seasonal snowcapped peaks and glaciated ranges. Prominent glaciers feeding upper Yamuna river basin are Yamunotri, Bandar Punch, Jamadar Bamak and Deokhera Bamak. Fan-shaped total basin area of its Himalayan reach is about 11400 km^2. The study area comprises of the main Yamuna river along with its major tributaries such as Pabbar, Tons, Aglar, Giri, Asan, Jalal, Bata etc. up to Hathini Kund Barrage in Haryana state. Many of these tributaries originate from snow covered areas of the Himalayas.

The upper basin area of Yamuna river mostly falls in the states of Uttarakhand and Himachal Pradesh, while a very small part of it falls in the states of Haryana and Uttar Pradesh. The basin area stretches from Yamunotri glacier in Uttarakhand to Hathini Kund Barrage in Haryana with a length of about 172 kilometers. From Yamunotri glacier, the Yamuna river flows in south-westerly direction through narrow and steep valleys before joining its principal tributary, the Tons, from the north at Kalsi. As the Tons drains a larger catchment area, it carries a greater volume of water than the main river Yamuna. From the west another important tributary, the Giri, joins the main river upstream of Paonta. The gradient of the upper Yamuna river basin is very steep and the entire geomorphology of the basin has been carved out by the erosive action of the river.

The climate of the basin is mostly subtropical monsoonal and is marked by strong seasonality. The temperature and rainfall regimes vary with altitude. The mean maximum temperature within the year varies from a low of 3.5ºC to a high of 34.7ºC. Normally, the monsoon sets in over parts of the study area by

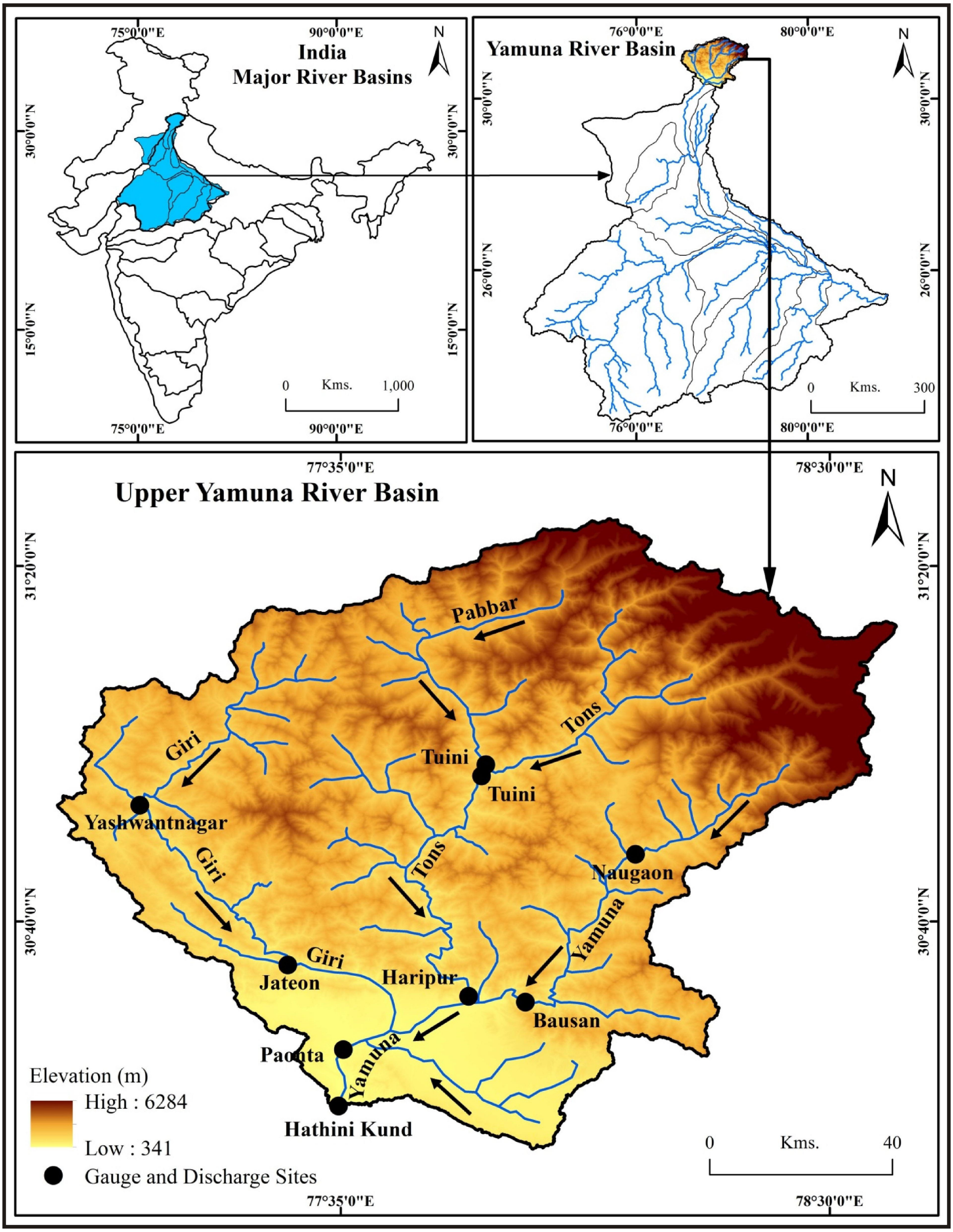
India
Major River Basins
75°0'0"E
90°0'0"E
30°0'0"N
15°0'0"N
N
0 Kms. 1,000
Yamuna River Basin
76°0'0"E
80°0'0"E
30°0'0"N
26°0'0"N
0 Kms. 300
Upper Yamuna River Basin
77°35'0"E
78°30'0"E
31°20'0"N
30°40'0"N
Pabbar
Tons
Giri
Tuini
Tuini
Yashwantnagar
Naugaon
Yamuna
Jateon
Haripur
Bausan
Paonta
Hathini Kund
Elevation (m)
High : 6284
Low : 341
Gauge and Discharge Sites
0 Kms. 40

Fig. 1

about the third week of June and withdraws by about the middle or third week of September. The mean annual rainfall of the catchment is about 140 cm of which 68 per cent is received during June to September months (monsoon season). The remaining rainfall occurs in winter season by western disturbances. Generally, October and November are the driest months of this region. During the non-monsoon period, stream flow is either due to glacier melt runoff or base flow. The soils in the region are highly variable and are composed of unconsolidated deposits of granites, slates, quartzites, and sandstone, with limestone bands of detrital origin. The natural vegetation in the region varies with altitude from semi-deciduous tropical in lower reaches to alpine in higher altitudes.

Database and Methodology

For an estimation of peak flood probabilities, a good and reliable database with respect to occurrence of past annual peak flood discharge series is necessary. Normally, a minimum of 30 years of data series without gaps is considered as a satisfactory time series for analysis. A smaller size of time series with breaks leads to improbability in extrapolation of estimates (Bobee et al., 1993; Onoz and Bayazit, 1995; Bobee and Robitaille, 1997). This study is primarily based on secondary sources of data. Annual peak flood discharge series data of nine gauge and discharge sites (Fig.1), have been acquired from Yamuna Basin Organization, Central Water Commission, New Delhi and Water Services Division, Irrigation and Water Resources Department, Dadupur, Yamuna Nagar, Haryana. Depending on availability, the length of annual peak flood discharge series data for the nine stations varies from 25 to 45 years (Table 1). The average area of the basin represented by each gauge and discharge site is about 1200 km^2. However, there are gaps in gauge and discharge sites network in the upper Yamuna river basin especially in north-eastern parts, where such network is very poor due to higher elevations (Fig.1). The measurement protocol at these sites is based on a standard stage-discharge relationship. The data sources referred above are the only reliable and official source for the study area. The collected data have been scrutinized carefully and considered reliable for projecting peak flood probabilities in the upper Yamuna river basin.

For this study, simple statistical techniques such as mean (Q_m), standard deviation (σ), coefficient of variation (C_v), and

Table 1
Upper Yamuna River Basin: Locational Characteristics of Gauge and Discharge Sites

Sites	District	State	River	Latitude	Longitude	Basin Area (km^2)	Elevation(m)	Time Period
Tuini (Pabbar)	Dehradun	Uttarakhand	Pabbar	30°57'37"N	77°51'13"E	1440	901	1977-2016
Tuini (Tons)	Dehradun	Uttarakhand	Tons	30°56'23"N	77°50'48"E	3438	901	1976-2014
Haripur	Dehradun	Uttarakhand	Tons	30°31'34"N	77°49'08"E	5141	495	1987-2016
Yashwantnagar	Sirmaur	Himachal Pradesh	Giri	30°53'12"N	77°12'22"E	1380	924	1977-2016
Jateon	Sirmaur	Himachal Pradesh	Giri	30°35'22"N	77°29'02"E	2395	670	1991-2015
Naugaon	Uttarkashi	Uttarakhand	Yamuna	30°47'30"N	78°08'07"E	1030	1138	1983-2016
Bausan	Dehradun	Uttarakhand	Yamuna	30°30'56"N	77°55'42"E	2143	616	1987-2015
Paonta	Sirmaur	Himachal Pradesh	Yamuna	30°25'31"N	77°35'31"E	11256	399	1979-2016
Hathini Kund	Yamunanagar	Haryana	Yamuna	30°18'51"N	77°35'06"E	11403	328	1975-2019

Source: Compiled by Authors.

coefficient of skewness (C_s) have been computed for each gauge and discharge site to derive the discharge characteristics of the upper Yamuna river basin. To detect the trends in time series of annual peak flood discharge and their deviation, simple linear regression (parametric) model has been applied. The slope explained the average rate of change over the study period. This model has been employed widely in time series investigations of hydrological studies. A detailed discussion of the model is available in Singh et al., 2020. The null hypothesis of no trend is rejected if the p value is lower than the level of significance. A trend has been considered significant, if the p value is less than or equal to 0.05. If not, there is not enough evidence of a meaningful trend at this significance level. The above-mentioned models have been executed by means of XLSTAT 2017 software.

The occurrence probabilities of peak floods have been computed by different probability distribution models that include normal and log-normal distributions (Rao and Hamed, 2000, Chow et al., 1988). In this study, two probability distribution models, namely GEV-I (Gumbel, 1941; 1958) and LP-III (Pearson, 1916; Chow et al., 1988; Rao and Hamed, 2000) have been employed to annual peak flood discharge series data for predicting the magnitude and frequency of discharges at 2-, 5-, 10-, 25-, 50-, 100- and 200- years return periods. Apart from this, the return periods of desired peak floods such as Q_m (mean annual peak flood discharge), Q_{lf} {(All floods that exceed the mean plus one standard deviation) ($>Q_m+1\sigma$)} (Hire, 2000), and Q_{max} (Observed maximum peak flood discharge) have been computed for the gauged period using GEV-I and LP-III models. These are the two most common and widely used statistical measures for flood frequency analysis for predicting and quantifying peak flood discharges at any given gauge and discharge site of a river for particular time intervals. GEV-I is also considered good for small sample size, while LP-III gives good results for large sample size (Kamal et al., 2017).

Additionally, Flash Flood Magnitude Index (FFMI), suggested by Kale (2003) has been computed for better understanding of long-term variability of annual peak flood discharge series (Q_{max}) over the upper Yamuna river basin. FFMI has been calculated from the standard deviation of the logarithms of annual peak flood discharge series. Also, flood indices (FI) have been computed as the ratios of estimated flood discharge (Q_T) to the mean of observed annual peak flood discharge series. FI is employed for flood regionalization of the watershed systems (Latt and Wittenberg, 2015).

Computation of GEV-I Probability Distribution Model

GEV-I statistical model is the most widely used to predict extreme hydrological events like floods. It is based on general model of peak events, particularly in the context of regionalization procedures and has been identified as a reasonable approach to predict the flood recurrence intervals (Latt and Wittenberg, 2015). In this study, the GEV-I probability distribution model has been employed for flood frequency analysis, because the peak flood discharge data cover a relatively longer record of about 25 years or more for different gauge and discharge sites in the study area. Mathematically, it is expressed as:

$$Q_T = Q_m\,(1+KC_v) \qquad (1)$$

where, Q_T is the estimated flood discharge with a return period of T years, C_v is the coefficient of variation, Q_m is the mean of annual peak flood discharge, K is the frequency factor represented by $(Y_T - \bar{Y})/\sigma$, in which $\bar{Y}T$ is the reduced variate for T years, is the mean value of reduced extremes and σ is the standard deviation of reduced extremes. Likewise, return periods for Q_m, Q_{lf} and Q_{max} have also been estimated for each gauge and discharge site. For this purpose, first of all $F(X)$ value has been computed by employing the equations (2), (3), and (4):

$$F(X) = e\left[-e^{-b(X-a)}\right] \quad (2)$$

where, $F(X)$ is the probability of an annual maximum peak flood $Q \leq X$ and a and b are two parameters related to the moments of the amount of annual peak flood discharge series. The parameters b and a have been obtained by using equations (3) and (4):

$$b = \frac{\pi}{\sigma Q\sqrt{6}} \quad (3)$$

$$a = Q_m - \frac{Y}{b} \quad (4)$$

The return period for desired discharges (Q_m, Q_{lf} and Q_{max}) has been computed by using equation (5):

$$T = \frac{1}{1 - F(X)} \quad (5)$$

where, $F(X)$ is the probability of an annual peak flood discharge obtained using equation (2).

Computation of LP-III Probability Distribution Model

Like GEV-I, LP-III probability distribution model has also been used widely for the estimation of peak floods and their return periods (Koutrouvelis and Canavos, 2000; Griffis and Stedinger, 2009; Bezak et al., 2014; Khattak et al., 2016; Kamal et al., 2017; Benameur et al., 2017). This distribution is often recommended for estimation of peak floods and has been used for design purposes as it provides accurate and reliable results. The steps involved in computing LP-III model are (i) annual peak flood discharge series values have been converted into logarithms using the equation $Y_i = log\ x_i$, (ii) from logarithms (Y_i), Mean ($\bar{y}$), standard deviation and skewness coefficient (C_s) have been computed, (iii) the logarithms of estimated flood discharges (Log Q_j) at 2-, 5-, 10-, 25-, 50-, 100- and 200-years return periods have been computed by using the equation Log $Q_j = \bar{y} + K_j C_s$, where K_j is a frequency factor which is a product of the return period and coefficient of skewness (C_s) and (4) the flood discharge (Q_j) has been computed by antilogarithms of Log Q_j. Likewise, the above statistical parameters have also been used to compute the return periods for Q_m, Q_{lf} and Q_{max}.

Computation of Goodness-of-Fit (GoF) Tests

Amongst the other distributions, the GoF tests are vital to check best-fit probability distribution at gauge and discharge sites. These tests have been applied widely in flood frequency analysis. The frequently used GoF tests are Kolmogorov-Smirnov (KS) and Anderson-Darling (AD) test. In this study, both KS and AD tests have been employed. The AD test is more appropriate than the KS test, because it gives more importance to the tails and also computes critical value on the basis of specific distribution (Ang and Tang, 2007; Kamal et al., 2017). The KS test measures the largest distance between an empirical Cumulative Distribution Function (CDF) and fitted CDF. However, AD test is a modification of the KS test and measures the discrepancy between the empirical and theoretical CDFs

(Ang and Tang, 2007). In this study, the results of both these tests have been obtained by using the EasyFit 5.6 software. Based on aforementioned details, a flowchart showing the overall methodology adopted for modeling of flood probability in the upper Yamuna river basin has been detailed in Fig. 2.

Results and Discussion

Characteristics of Annual Peak Flood Discharge Series

Table 2 shows the annual peak flood discharge series characteristics such as maximum, minimum and mean values, standard deviations, coefficient of variability, coefficient of skewness, ratio of maximum (Q_{max}) and mean (Q_m) flood, observed specific discharge and flash flood magnitude index of the upper Yamuna river basin. The highest Q_{max} has been recorded at Hathini Kund gauge and discharge site followed by Paonta, Haripur and Jateon. Similarly, Q_{min} has been recorded lowest at Yashwantnagar gauge and discharge site followed by Tuini (Pabbar), Haripur and Jateon. The Q_m of the whole upper Yamuna river basin has been observed to the tune of 1704.11 m^3/s with a standard deviation of 1229.79 m^3/s. The highest averages of the Q_m are 8,152, 2,581, 1,168 and 915 m^3/s with a standard deviation of 6,174, 1,455, 1,006 and 803 m^3/s for Hathini Kund, Paonta, Haripur and Jateon gauge and discharge sites, respectively. Whereas, the lowest averages of the Q_m are 240, 247 and 393 m^3/s for Tuini (Pabbar), Naugaon and Yashwantnagar gauge and discharge sites, respectively. Interestingly, the Q_{max} is more than Q_m for 17 and 16 times at Tuini (Tons) and Hathini Kund gauge and discharge sites, respectively.

The analysis of Q_{max} reveals a high inter annual variability as the C_v lies between 47 per cent at Naugaon gauge and discharge site to 104 per cent at Yashwantnagar with a mean value of 71 per cent for the whole upper Yamuna river basin. A high variability of Q_{max} presumably may be an effect of regional climate as well as annual changes in intensity of monsoon rainfall and snow melt runoff contribution. Delgado et al. (2010) have observed that the variation of peak floods in monsoon dominated rivers of Southeast Asia occurs due to heavy rainfall. However, the Cs varies between a low of 0.93 at Bausan to a high of 1.97 at Jateon gauge and discharge sites. The

Table 2

Upper Yamuna River Basin: Statistical Characteristics of Annual Peak Flood Discharge Series

Sites	N	Q_{max} (m^3/s)	Q_{min} (m^3/s)	Q_m (m^3/s)	S. D. (σ)	Q_{1f} (m^3/s)	N (Q_{max}>Q_m)	N (Q_{max}>Q_{1f})	C_V	C_s	Q_{sd} ($m^3/s/km^2$)	Q_{max}/Q_m ratio	FFMI
Tuini (Pabbar)	40	685	47	240.14	163.70	403.84	11	6	0.68	1.49	0.48	2.85	0.27
Tuini (Tons)	39	1719	159	727.49	417.10	1144.59	17	6	0.57	1.13	0.50	2.36	0.25
Haripur	30	4498	97	1168.42	1005.59	2174.01	12	3	0.86	1.95	0.87	3.85	0.41
Yashwantnagar	40	1788	40	392.75	409.92	802.67	11	6	1.04	1.94	1.30	4.55	0.41
Jateon	25	3309	105	914.75	803.45	1718.20	10	2	0.88	1.97	1.38	3.62	0.38
Naugaon	34	841	119	346.72	161.53	508.25	12	4	0.47	1.43	0.82	2.43	0.18
Bausan	29	1794	202	814.53	478.67	1293.19	10	5	0.59	0.93	0.84	2.20	0.26
Paonta	38	7196	567	2580.63	1454.59	4035.22	15	4	0.56	1.36	0.64	2.79	0.26
Hathini Kund	45	23448	1377	8151.53	6173.58	14325.11	16	9	0.76	1.11	2.06	2.88	0.32
Whole basin	**-**	**5031**	**301**	**1704.11**	**1229.79**	**2933.90**	**13**	**5**	**0.71**	**1.48**	**0.99**	**3.06**	**0.30**

Source: Compiled by Authors. N = Number of Years.

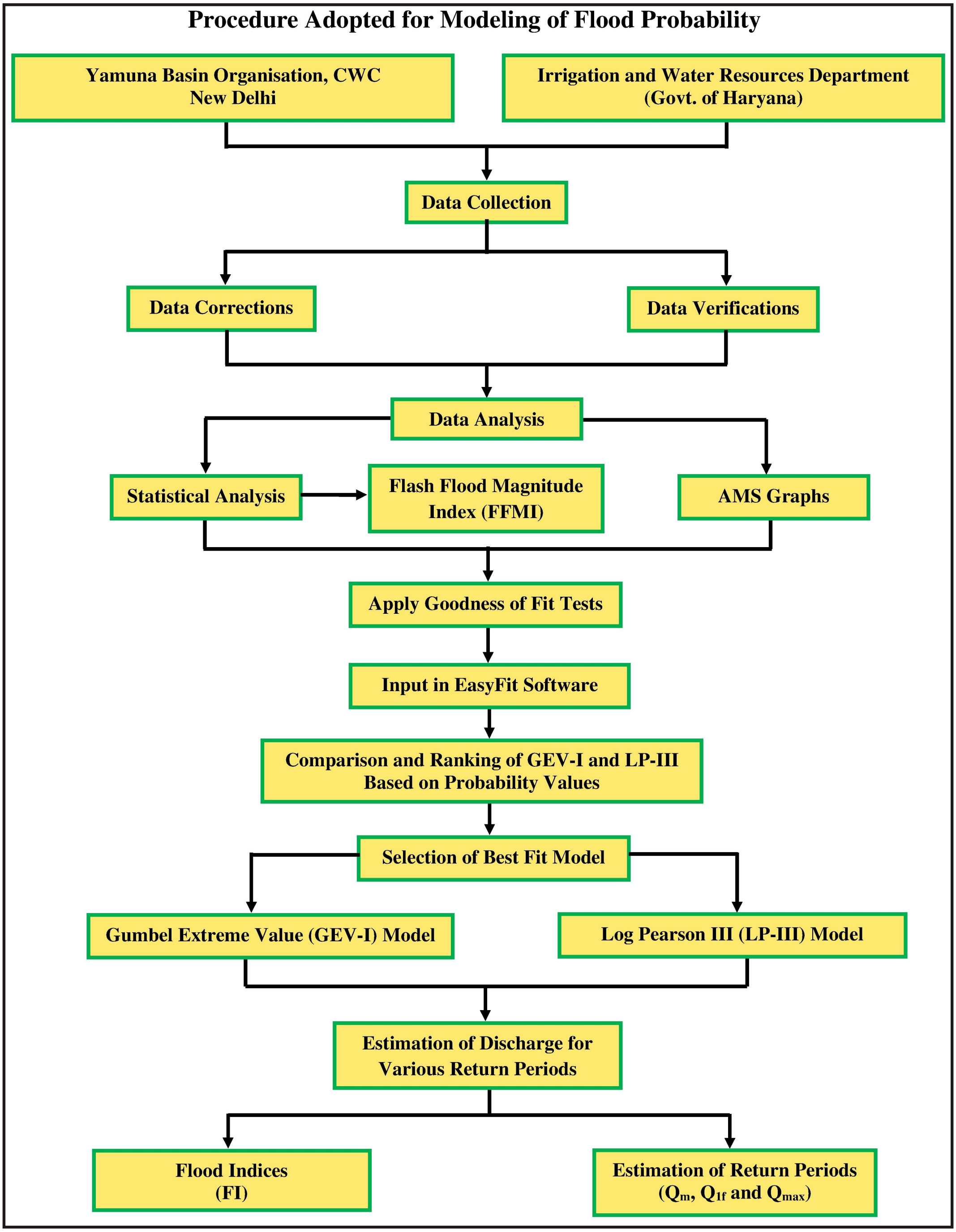
Procedure Adopted for Modeling of Flood Probability
Yamuna Basin Organisation, CWC New Delhi
Irrigation and Water Resources Department (Govt. of Haryana)
Data Collection
Data Corrections
Data Verifications
Data Analysis
Statistical Analysis
Flash Flood Magnitude Index (FFMI)
AMS Graphs
Apply Goodness of Fit Tests
Input in EasyFit Software
Comparison and Ranking of GEV-I and LP-III Based on Probability Values
Selection of Best Fit Model
Gumbel Extreme Value (GEV-I) Model
Log Pearson III (LP-III) Model
Estimation of Discharge for Various Return Periods
Flood Indices (FI)
Estimation of Return Periods (Q_m, Q_{1f} and Q_{max})

Fig. 2

Cs values more than 1 at all gauge and discharge sites over the basin except Bausan indicate that at least two or more high magnitude floods have occurred during the gauging period at these sites. The ratio of observed Q_{max} and Q_m indicates that the largest ever recorded flood during the study period at Tuini (Pabbar), Tuini (Tons), Naugaon, Bausan, Paonta and Hathini Kund gauge and discharge sites is two times larger, while for Haripur, Jateon and Yashwantnagar sites it is about three-to-four times larger than the Q_m (Table 2). The average specific discharge (Q_{sd}) has ranged between 0.48 $m^3/s/km^2$ at Tuini Pabbar to 2.06 $m^3/s/km^2$ at Hathini Kund in the basin.

Fig. 3 demonstrates the FFMI against the ratios of Q_{max} and Q_m at different gauge and discharge sites, which vary between 0.18 to 0.41. Higher the values of FFMI, larger are the floods, leading to major hydro geomorphic changes (Patton and Baker, 1976; Kochel, 1988). The results of this study reveal an inter-annual variability in peak floods, which is almost consistent across all the gauge and discharge sites (Table 2). Fig. 4 exhibits the distribution of standardized Q_{max} within the basin area with reference to all gauge and discharge sites. The box plots have revealed that the Q_{max} with respect to basin area is highest at Hathini Kund gauge and discharge site followed by Jateon and Yashwantnagar with the lowest being at Tuini (Pabbar) gauge and discharge site. These results reveal that the incidence of flood generation enhances with the increase in basin area.

Time Series Analysis of Floods

Fig. 5 exhibits the annual Q_{max} at nine gauge and discharge sites in the study area. These time-series plots show a spatio-temporal

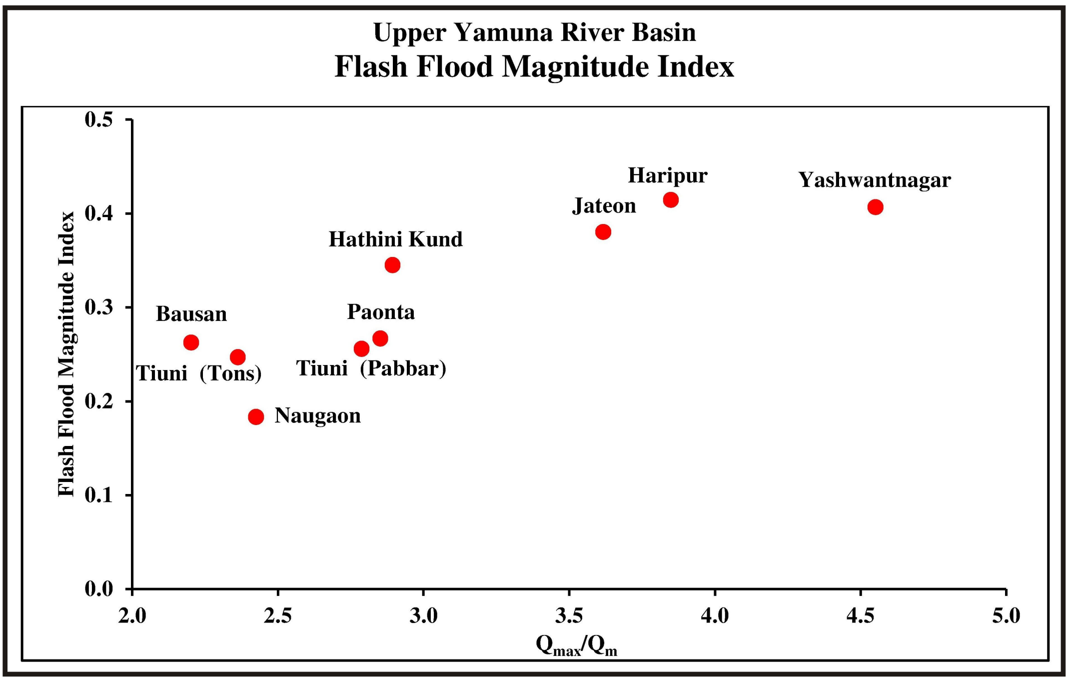

Fig. 3

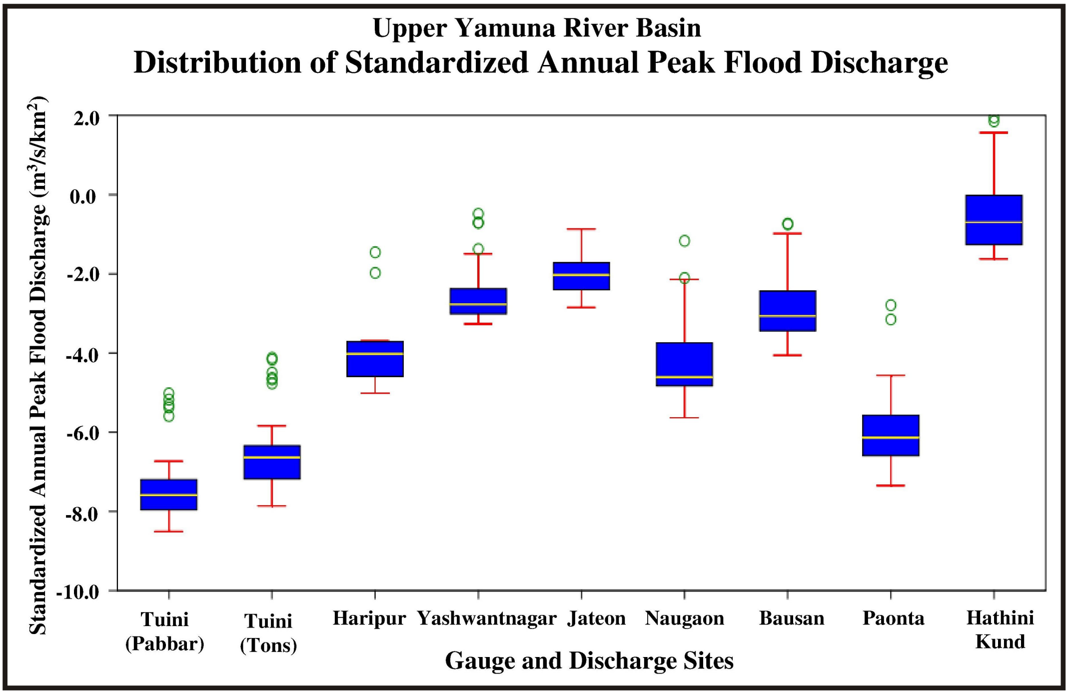
Upper Yamuna River Basin
Distribution of Standardized Annual Peak Flood Discharge
Standardized Annual Peak Flood Discharge ($m^3/s/km^2$)
2.0
0.0
-2.0
-4.0
-6.0
-8.0
-10.0
Tuini (Pabbar)
Tuini (Tons)
Haripur
Yashwantnagar
Jateon
Naugaon
Bausan
Paonta
Hathini Kund
Gauge and Discharge Sites

Fig. 4

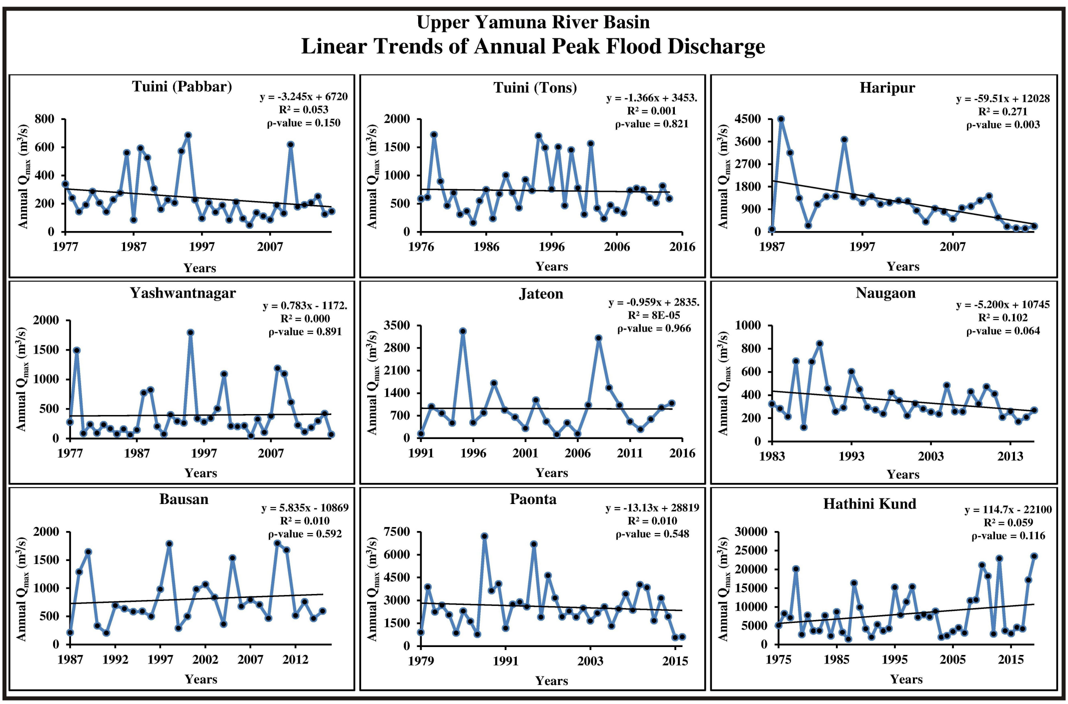
Upper Yamuna River Basin
Linear Trends of Annual Peak Flood Discharge
Tuini (Pabbar)
y = -3.245x + 6720
R^2 = 0.053
ρ-value = 0.150
Tuini (Tons)
y = -1.366x + 3453.
R^2 = 0.001
ρ-value = 0.821
Haripur
y = -59.51x + 12028
R^2 = 0.271
ρ-value = 0.003
Yashwantnagar
y = 0.783x - 1172.
R^2 = 0.000
ρ-value = 0.891
Jateon
y = -0.959x + 2835.
R^2 = 8E-05
ρ-value = 0.966
Naugaon
y = -5.200x + 10745
R^2 = 0.102
ρ-value = 0.064
Bausan
y = 5.835x - 10869
R^2 = 0.010
ρ-value = 0.592
Paonta
y = -13.13x + 28819
R^2 = 0.010
ρ-value = 0.548
Hathini Kund
y = 114.7x - 22100
R^2 = 0.059
ρ-value = 0.116
Annual Q_{max} (m^3/s)
Years

Fig. 5

variation with some of the prominent peaks of flood discharge during the gauging period at all sites. Decreasing trends with negative slopes have been detected in annual Q_{max} at all gauge and discharge sites except at Yashwantnagar, Bausan and Hathini Kund sites, which shows a positive trend in annual Q_{max}. These increasing trends at Yashwantnagar, Bausan and Hathini Kund gauge and discharge sites approve the hypotheses of climate change, indicating that the area will experience more extreme events in future. Apart from this, significant decreasing trends have been detected only at Haripur gauge and discharge site in the Q_{max} $(p = 0.003)$ (Fig. 5). Meanwhile, Hathini Kund gauge and discharge site in the basin has witnessed comparatively higher Q_m and Q_{max} than other gauge and discharge sites. Hathini Kund gauge and discharge site has recorded the largest ever peak flood discharges of 23,448, 22,837, 21,082 and 20,083 m^3/s in the years 2019, 2013, 2010 and 1978, respectively (Fig. 5). These largest ever recorded peak flood discharges at Hathini Kund are associated with heavy to very heavy rainfall due to monsoons in the upper reaches of the basin.

Apart from above, the plots of deviation with respect to Q_{max} from the Q_m have shown reciprocal trends as that of Q_{max} with a large inter-annual variability at all gauge and discharge sites (Fig. 6). Interestingly, Haripur and Naugaon gauge and discharge sites have witnessed significant positive trends of deviation at 95 per cent level of significance, whereas Yashwantnagar gauge and discharge site has recorded a significant decreasing trend of deviation from Q_m $(p = 0.000)$.

Additionally, the quadratic trend model

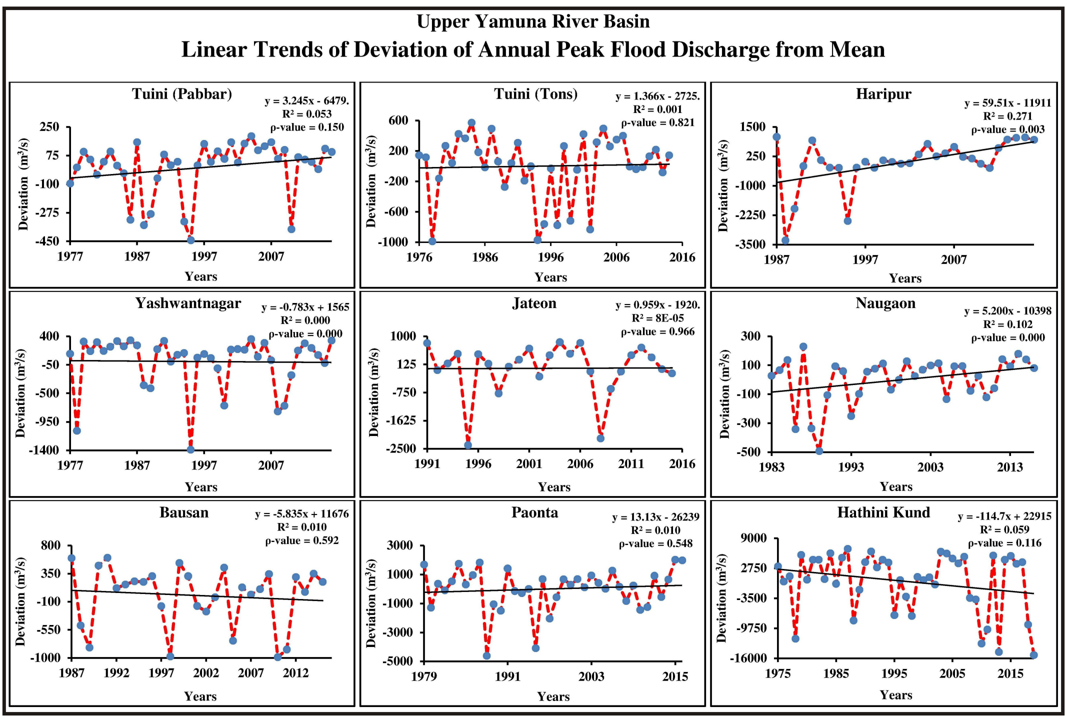

Fig. 6

projection plot of annual peak flood discharge has been graphically shown in the form of time series plots of Q_{max} forecast at nine gauge and discharge sites based on the observed Q_{max} value for the study period (Fig. 7). It has been observed from these plots that the frequency and magnitude of Q_{max} is likely to increase only at Hathini Kund gauge and discharge site in future as a result of climate variability. Bhat et al. (2019b) have reported similar results for river Jhelum in Kashmir basin. In the given scenario, any contemplation aiming at probabilistic assessment may be potentially valuable from the perspective of research and for regional flood hazard mitigation (Bhat et al., 2019b).

Flood Frequency Analysis

Flood frequency analysis is a statistical method for determining the hydrological behavior of rivers, because of its diverse existence and multiple uncertainties in the path (Bhat et al., 2019a). Based on GEV-I and LP-III distribution models, flood frequency analysis has been carried out to construct the frequency distributions of Q_{max} as a function of recurrence interval at nine gauge and discharge sites (Table 3). The expected mean and the expected standard deviation values for GEV-I probability distribution are almost constant. However, for LP-III probability distribution, the mean value varies between 2.30 to 3.79, while the standard deviation varies between 0.18 to 0.41. Interestingly, C_s values for the distribution are negatively skewed for Tuini (Tons), Haripur, Jateon, Bausan and Paonta gauge and discharge sites, whereas Cs values for the distribution are positively skewed for Tuini

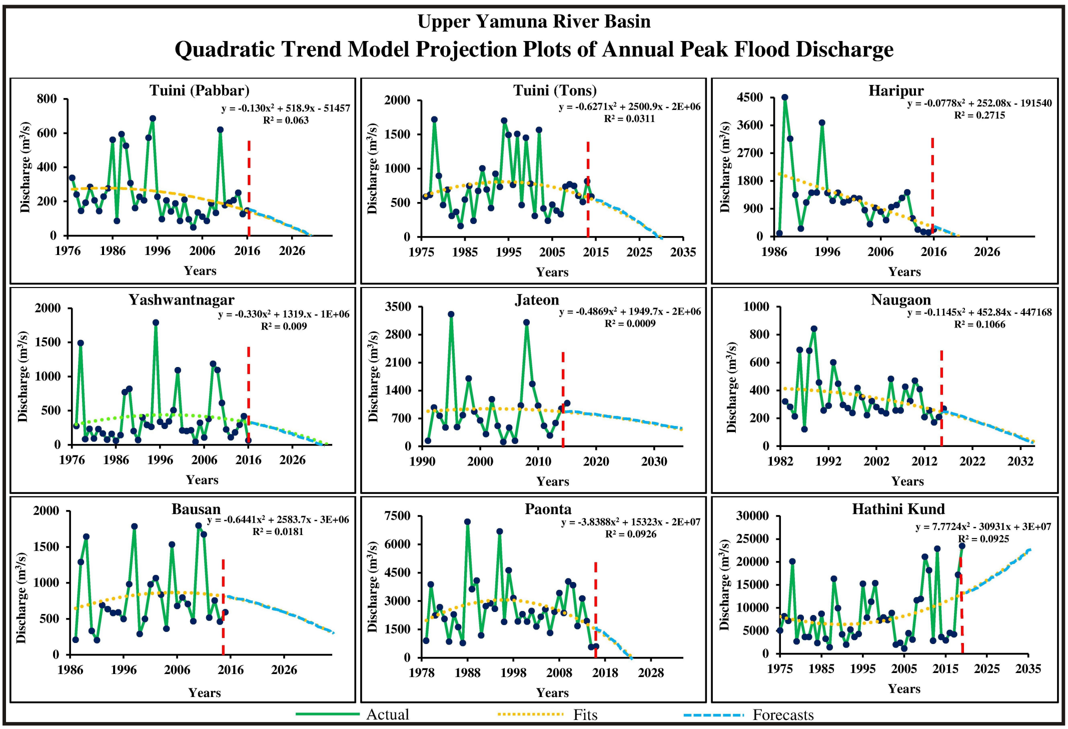

Fig. 7

Table 3
Upper Yamuna River Basin: Parameters for GEV-I and LP-III Distribution Models

Parameters	Tuini (Pabbar)	Tuini (Tons)	Haripur	Yashwantnagar	Jateon	Naugaon	Bausan	Paonta	Hathini Kund
GEV-I									
Mean discharge (m^3/s)	240.14	727.49	1168.42	392.75	914.75	346.72	806.76	2580.63	8100.64
Standard deviation (σ)	163.70	417.10	1005.59	409.92	803.45	161.53	492.86	1454.59	6223.12
Expected mean ($\overline{Y}$)	0.54	0.54	0.54	0.54	0.53	0.54	0.54	0.54	0.55
Expected standard deviation (σ_n)	1.14	1.14	1.11	1.14	1.09	1.13	1.11	1.14	1.15
LP-III									
Mean values	2.30	2.80	2.91	2.41	2.82	2.50	2.83	3.34	3.79
Standard deviation (σ)	0.27	0.25	0.41	0.41	0.38	0.18	0.26	0.26	0.32
Coefficient of skewness (C_s)	0.23	-0.12	-0.65	0.18	-0.37	0.30	-0.13	-0.49	0.10

Source: Compiled by Authors.

(Pabbar), Yash-wantnagar, Naugaon and Hathini Kund (Table 3). Further, to confirm whether the Q_{max} follows the GEV-I distribution or not, a plot has been made between the Q_{max} and its reduced variate for all gauge and discharge sites (Fig. 8). These plots reveal that Q_{max} follows a linear relationship (best fit) with the reduced variate over most of the gauge and discharge sites. However, this fitting is better for Hathini Kund, Naugaon, Bausan and Paonta gauge and discharge sites, but not so good for the remaining gauge and discharge sites.

The computation of variables for the

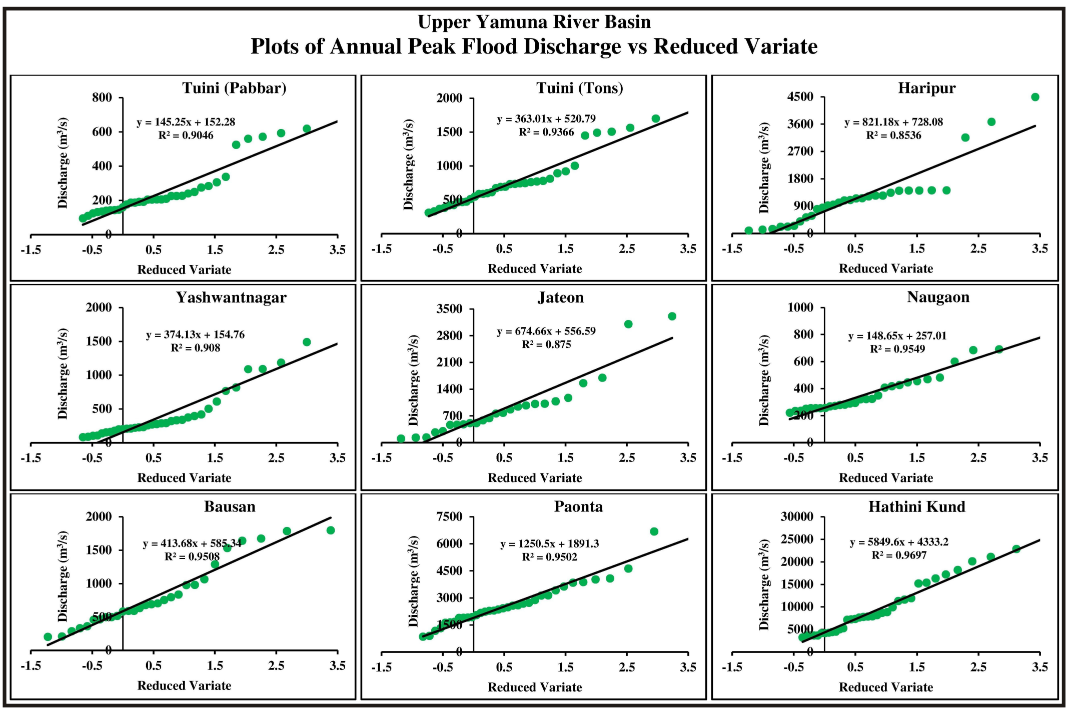

Fig. 8

derivation of estimated discharges for all floods at different gauge and discharge sites have been predicted for 2-, 5-, 10-, 25-, 50-, 100- and 200- years return periods using GEV-I and LP-III distribution models (Table 4). A comparison of the estimated discharges for 25-year return periods based on GEV-I and LP-III distribution models indicates that the estimated discharge (1700 m^3/s) calculated by using GEV-I distribution model is closer to the observed Q_{max} (1719 m^3/s) at Tuini (Tons) gauge and discharge site. Similarly, the estimated discharge for the same return periods (23,935 m^3/s) calculated by using LP-III distribution model is closer to the observed Q_{max} (23,448 m^3/s) at Hathini Kund gauge and discharge site. Apart from this, the estimated discharge for 50-year return periods at Naugaon gauge and discharge site using GEV-I distribution model (829 m^3/s) is also very close to the observed Q_{max} (841 m^3/s) as compared to LP-III distribution model (806 m^3/s). Likewise, the estimated discharge for the same return period (3292 m^3/s) calculated by using LP-III distribution model is closer to the observed Q_{max} (3309 m^3/s) at Jateon gauge and discharge site. This implies that GEV-I distribution has more significant implication at Tuini (Tons) and Naugaon gauge and discharge sites for projecting flood for hydraulic structures, whereas LP-III distribution model is more appropriate for Jateon and Hathini Kund sites. The flood frequency estimates and the discharge magnitude of various floods obtained from GEV-I and LP-III distribution models in the upper Yamuna river basin have been shown in Fig. 9. The probability distribution used for the estimation of return periods with the magnitude of estimated discharge shows that the exceedance probability decreases with increasing time.

A comparison of estimated discharges with various return periods by GEV-I and LP-III distribution models at different gauge and discharge sites has been exhibited graphically in Fig. 10. These plots show that the estimated discharges for the 2-year return period are less than the Q_m with GEV-I and LP-III distribution models all over the basin. Similarly, the estimated discharges for 5-year return periods are below than Q_{If} with GEV-I and LP-III distribution model at all gauge and discharge sites. While, estimated discharges for 10-year return periods are fairly close to the Q_{If} all over the basin. Interestingly, for 50- and 100-year return periods, the estimated discharge is almost equal or close to the observed Q_{max} with GEV-I and LP-III distribution model in the study area (Fig. 10).

Apart from above, the plots have also been drawn to find out the relationship between the observed Q_{max} and the estimated discharge for 25-, 50-, 100- and 200-year return periods in the upper Yamuna river basin by using GEV-I and LP-III (Fig. 11). The r^2 value of these plots suggests that there is a positive correlation between observed Q_{max} and the estimated discharges at each gauge and discharge site in the entire basin. Therefore, it is concluded that the GEV-I and LP-III distribution models can be considered satisfactory for flood modeling in the upper Yamuna river basin. These results are in correspondence with some previous studies (Bhat et al., 2019a; Pawar et al., 2020).

Return Period Analysis for Q_m, Q_{if} and Q_{max}

The estimation of large magnitude floods return period is imperative in the magnitude-frequency analysis, because these floods are more dangerous than mean annual flows in a basin as these occur after an interval of several years (Hire, 2000). Therefore, in this

Table 4
Upper Yamuna River Basin: Flood Frequency Estimates with GEV-I and LP-III Distribution Models

Return Period	GEV-I				LP-III			
	Reduced Variate	Frequency Factor	Estimated Discharge (m^3/s)	FI	Frequency Factor	Log of Estimated Discharge	Estimated Discharge (m^3/s)	FI
Tuini (Pabbar)								
2	0.37	-0.16	215	0.89	-0.04	2.29	194	0.81
5	1.50	0.84	377	1.57	0.83	2.52	330	1.37
10	2.25	1.50	485	2.02	1.30	2.65	442	1.84
25	3.20	2.33	621	2.59	1.83	2.79	611	2.54
50	3.90	2.94	722	3.01	2.18	2.88	756	3.15
100	4.60	3.55	822	3.42	2.50	2.96	921	3.83
200	5.30	4.16	922	3.84	2.79	3.04	1106	4.61
Tuini (Tons)								
2	0.37	-0.15	663	0.91	0.06	2.81	646	0.89
5	1.50	0.84	1078	1.48	0.87	3.01	1023	1.41
10	2.25	1.50	1353	1.86	1.26	3.11	1282	1.76
25	3.20	2.33	1700	2.34	1.67	3.21	1613	2.22
50	3.90	2.95	1958	2.69	1.92	3.27	1860	2.56
100	4.60	3.56	2213	3.04	2.14	3.32	2106	2.90
200	5.30	4.17	2468	3.39	2.33	3.37	2353	3.23
Haripur								
2	0.37	-0.15	1015	0.87	0.11	2.95	899	0.77
5	1.50	0.87	2040	1.75	0.86	3.26	1839	1.57
10	2.25	1.54	2718	2.33	1.19	3.40	2531	2.17
25	3.20	2.39	3575	3.06	1.51	3.53	3423	2.93
50	3.90	3.03	4211	3.60	1.69	3.61	4079	3.49
100	4.60	3.65	4842	4.14	1.84	3.67	4713	4.03
200	5.30	4.28	5471	4.68	1.97	3.73	5325	4.56
Yashwantnagar								
2	0.37	-0.16	329	0.84	-0.03	2.39	248	0.63
5	1.50	0.84	736	1.87	0.83	2.74	556	1.42
10	2.25	1.50	1006	2.56	1.30	2.94	861	2.19
25	3.20	2.33	1346	3.43	1.81	3.14	1391	3.54
50	3.90	2.94	1599	4.07	2.15	3.28	1908	4.86
100	4.60	3.55	1850	4.71	2.46	3.41	2548	6.49
200	5.30	4.16	2100	5.35	2.74	3.52	3332	8.48
Jateon								
2	0.37	-0.15	794	0.87	0.06	2.84	690	0.75
5	1.50	0.89	1628	1.78	0.85	3.14	1384	1.51
10	2.25	1.58	2181	2.38	1.24	3.29	1934	2.11
25	3.20	2.44	2879	3.15	1.62	3.43	2704	2.96
50	3.90	3.09	3396	3.71	1.84	3.52	3292	3.60
100	4.60	3.73	3910	4.27	2.05	3.60	3963	4.33
200	5.30	4.37	4422	4.83	2.23	3.67	4633	5.06
Naugaon								
2	0.37	-0.15	322	0.93	-0.05	2.49	310	0.89
5	1.50	0.85	485	1.40	0.82	2.65	449	1.29
10	2.25	1.52	592	1.71	1.31	2.74	550	1.59
25	3.20	2.36	728	2.10	1.85	2.84	692	1.99
50	3.90	2.99	829	2.39	2.21	2.91	806	2.32
100	4.60	3.61	929	2.68	2.54	2.97	927	2.67
200	5.30	4.23	1029	2.97	2.86	3.02	1058	3.05
Bausan								
2	0.37	-0.15	732	0.91	0.02	2.84	690	0.85
5	1.50	0.87	1236	1.53	0.85	3.06	1137	1.41
10	2.25	1.55	1569	1.95	1.27	3.17	1465	1.82
25	3.20	2.40	1991	2.47	1.71	3.28	1911	2.37
50	3.90	3.04	2304	2.86	1.98	3.35	2262	2.80
100	4.60	3.67	2614	3.24	2.23	3.42	2627	3.26
200	5.30	4.29	2923	3.62	2.46	3.48	3008	3.73
Paonta								
2	0.37	-0.15	2355	0.91	-0.04	3.33	2161	0.84
5	1.50	0.84	3806	1.47	0.83	3.56	3599	1.39
10	2.25	1.50	4767	1.85	1.30	3.68	4757	1.84
25	3.20	2.34	5981	2.32	1.82	3.81	6471	2.51
50	3.90	2.96	6881	2.67	2.17	3.90	7943	3.08
100	4.60	3.57	7775	3.01	2.49	3.98	9581	3.71
200	5.30	4.18	8666	3.36	2.79	4.06	11414	4.42
Hathini Kund								
2	0.37	-0.15	7188	0.89	-0.02	3.79	6121	0.76
5	1.50	0.83	13263	1.64	0.84	4.07	11669	1.44
10	2.25	1.48	17284	2.13	1.29	4.22	16479	2.03
25	3.20	2.30	22367	2.76	1.79	4.38	23935	2.95
50	3.90	2.91	26137	3.23	2.11	4.48	30546	3.77
100	4.60	3.52	29579	3.69	2.40	4.58	38136	4.71
200	5.30	4.12	33608	4.15	2.67	4.67	46792	5.78

Source: Compiled by Authors.

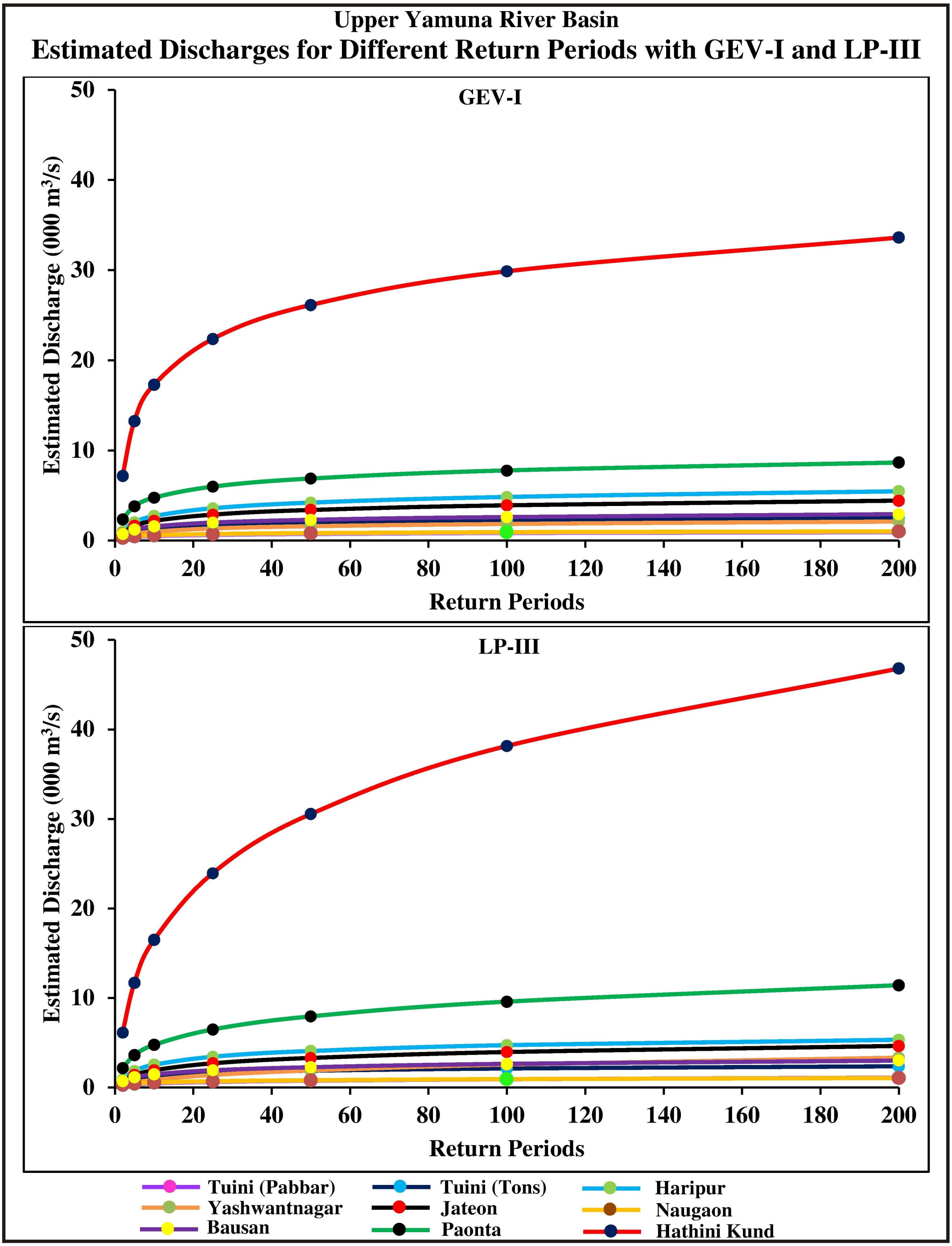
Upper Yamuna River Basin
Estimated Discharges for Different Return Periods with GEV-I and LP-III
GEV-I
LP-III
Estimated Discharge (000 m³/s)
Return Periods
0
10
20
30
40
50
0
20
40
60
80
100
120
140
160
180
200
Tuini (Pabbar)
Yashwantnagar
Bausan
Tuini (Tons)
Jateon
Paonta
Haripur
Naugaon
Hathini Kund

Fig. 9

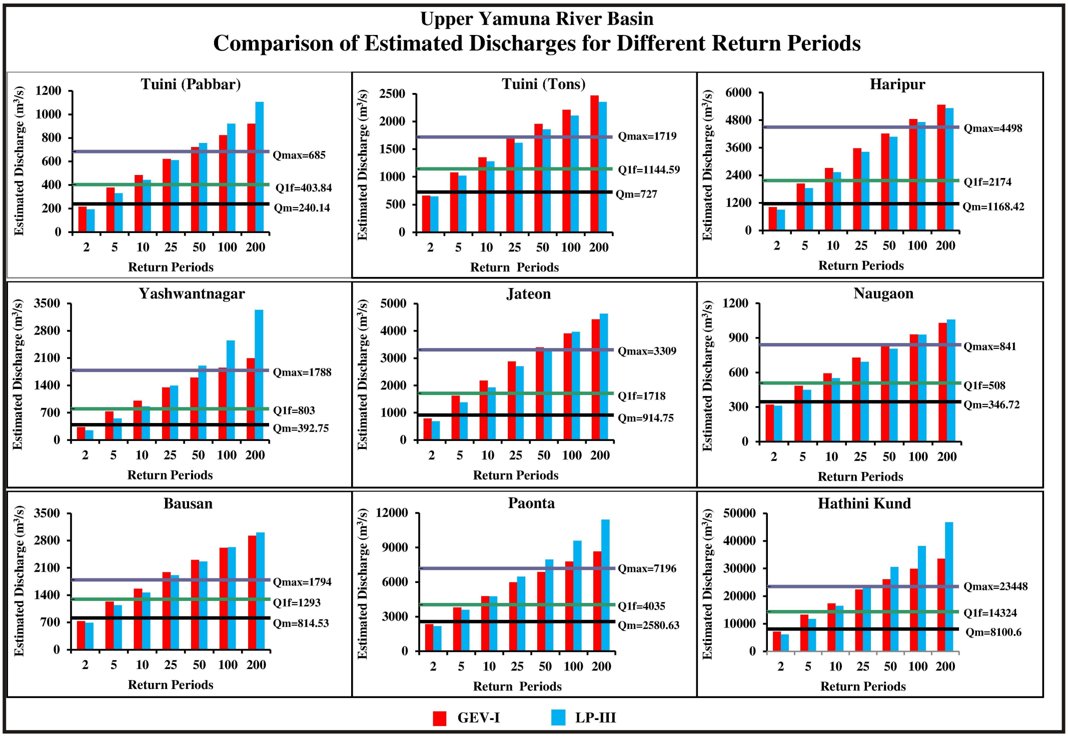

Fig. 10

study, an attempt has been made for estimation of return periods with respect to Q_m, Q_{1f} and Q_{max} for all gauge and discharge sites by using the GEV-I and LP-III distribution models (Table 5). The results of GEV-I distribution model reveal that the return periods for Q_m and Q_{1f} are 2.3- and 6.9-years, respectively for all gauge and discharge sites. However, the return period for Q_{max} varies significantly from 88-years (highest) for Yashwantnagar gauge and discharge site and 18-years (lowest) for Bausan. The maximum discharge ever recorded throughout the study period was 23,448 m^3/s at Hathini Kund gauge and discharge site which has a return period of 32-years when using the GEV-I distribution model, but only 24-years when using the LP-III distribution model. Furthermore, the LP-III distribution model results show that the return periods for Q_m, Q_{1f} and Q_{max} vary all over the basin. The Q_m return period varies between 2.7-years (lowest) for Tuini (Tons) gauge and discharge site to 3.4-years (highest) at Yashwantnagar. The return periods of Q_{1f} have ranged from 7.01-years (Paonta) to 9.0-years (Yashwant-nagar). However, the Q_{max} return periods have ranged between 83-years for Haripur gauge and discharge site (highest) to 21-years at Bausan (lowest).

Goodness-of-Fit Test Analysis

The application of GoF test is the most important step to find out the best-fit flood probability model at each gauge and discharge site over the basin. Therefore, GoF test, namely, KS and AD have been employed all over the basin using EasyFit software. In this study, all the probability values have been procured

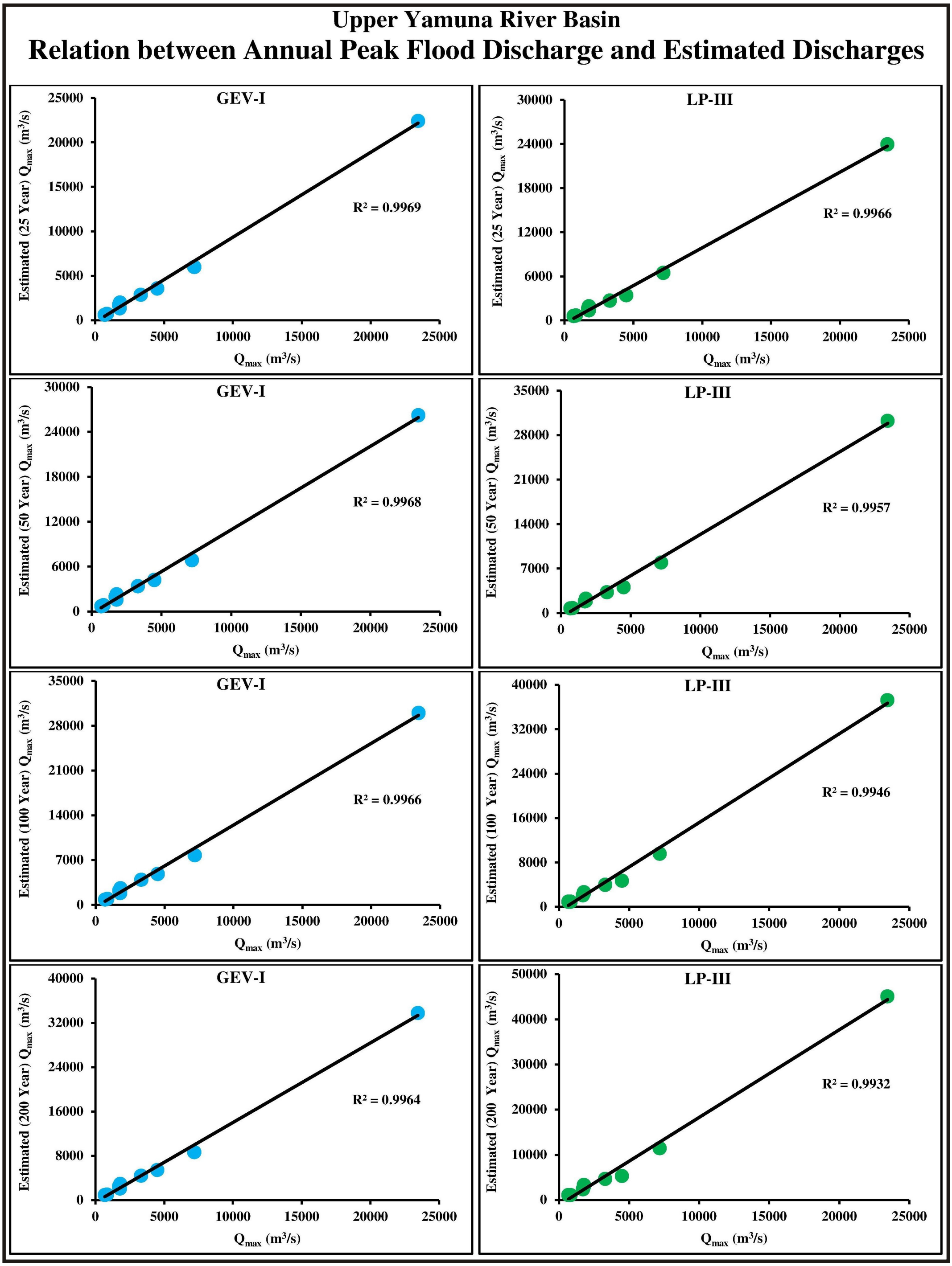
Upper Yamuna River Basin
Relation between Annual Peak Flood Discharge and Estimated Discharges
GEV-I
R² = 0.9969
Estimated (25 Year) Qmax (m³/s)
Qmax (m³/s)
LP-III
R² = 0.9966
GEV-I
R² = 0.9968
Estimated (50 Year) Qmax (m³/s)
LP-III
R² = 0.9957
GEV-I
R² = 0.9966
Estimated (100 Year) Qmax (m³/s)
LP-III
R² = 0.9946
GEV-I
R² = 0.9964
Estimated (200 Year) Qmax (m³/s)
LP-III
R² = 0.9932

Fig. 11

Table 5
Upper Yamuna River Basin: Return Periods of Q_m, Q_{1f} and Q_{max} with GEV-I and LP-III Distribution Models

Sites	Discharge(m^3/s)	Return Period (GEV-I)	Return Period (LP-III)
Tuini (Pabbar)	Q_m = 240.13	2.33	3.10
	Q_{1f} = 403.84	6.93	8.30
	Q_{max} = 685	42.00	38.00
Tuini (Tons)	Q_m = 727.49	2.33	2.70
	Q_{1f} = 1144.59	6.93	7.40
	Q_{max} = 1719	27.00	36.00
Haripur	Q_m = 1168.41	2.33	2.90
	Q_{1f} = 2174	6.93	7.50
	Q_{max} = 4498	73.00	83.00
Yashwantnagar	Q_m = 392.75	2.33	3.40
	Q_{1f} = 802.67	6.93	9.00
	Q_{max} = 1788	88.00	44.00
Jateon	Q_m = 914.74	2.33	3.00
	Q_{1f} = 1718.19	6.93	8.00
	Q_{max} = 3309	46.00	51.00
Naugaon	Q_m = 346.72	2.33	2.80
	Q_{1f} = 508.24	6.93	8.30
	Q_{max} = 841	56.00	65.00
Bausan	Q_m = 806.76	2.33	2.90
	Q_{1f} = 1293.19	6.82	7.40
	Q_{max} = 1794	18.00	21.00
Paonta	Q_m = 2580.63	2.33	2.90
	Q_{1f} = 4035.22	6.93	7.00
	Q_{max} = 7196	68.00	38.00
Hathini Kund	Q_m = 8152.00	2.33	3.05
	Q_{1f} = 14325.11	6.93	8.00
	Q_{max} = 23448	32.00	24.00

Source: Compiled by Authors.

by contemplating the critical value at 95% confidence level *(α = 0.05)*. The ranks have been given to the GEV-I and LP-III distribution models by matching their calculated probability values. The rank 1 illustrates acceptance level (best-fit), while rank 2 indicates rejection level of the model (Table 6). Interestingly, the results of the KS and AD test show the same ranking for the GEV-I and LP-III model at every gauge and discharge site. The results reveal that the GEV-I distribution model is best suited (accepted) for Paonta gauge and

Table 6
Upper Yamuna River Basin: Goodness-of-Fit (GoF) Tests Results of GEV-I and LP-III Distribution Models

Sites	Distribution	Kolmogorov-Smirnov (KS) Tests				Anderson-Darling (AD) Tests			
		Statistic	Reject	Critical Value at 0.05	Rank	Statistic	Reject	Critical Value at 0.05	Rank
Tuini (Pabbar)	GEV-I	0.1635	No	0.2101	2	1.4473	No	2.5018	2
	LP-III	0.0994	No		1	0.5091	No		1
Tuini (Tons)	GEV-I	0.1244	No	0.2127	2	0.5850	No	2.5018	2
	LP-III	0.0986	No		1	0.3806	No		1
Haripur	GEV-I	0.2339	No	0.2417	2	1.1787	No	2.5018	2
	LP-III	0.2018	No		1	1.0123	No		1
Yashwantnagar	GEV-I	0.1853	No	0.2101	2	2.2339	No	2.5018	2
	LP-III	0.0791	No		1	0.2798	No		1
Jateon	GEV-I	0.1508	No	0.2640	2	0.7997	No	2.5018	2
	LP-III	0.1301	No		1	0.3515	No		1
Naugaon	GEV-I	0.1391	No	0.2274	2	0.7521	No	2.5018	2
	LP-III	0.1058	No		1	0.4456	No		1
Bausan	GEV-I	0.1080	No	0.2457	2	0.4680	No	2.5018	2
	LP-III	0.0854	No		1	0.2804	No		1
Paonta	GEV-I	0.0950	No	0.2154	1	0.3070	No	2.5018	1
	LP-III	0.1055	No		2	0.3814	No		2
Hathini Kund	GEV-I	0.1363	No	0.1983	2	1.0349	No	2.5018	2
	LP-III	0.0913	No		1	0.3737	No		1

Source: Compiled by Authors.

discharge site, whereas LP-III distribution model is best fit (accepted) for the remaining gauge and discharge sites.

After accomplishing the GoF tests, the CDF and P-P plot diagrams have been prepared for all gauge and discharge sites to check the suitability of results. Fig. 12a and b demonstrate the CDF, whereas Fig. 13a and b display the P-P plot diagrams using GEV-I and LP-III distribution models. The results of these models are considered to be the best-fit if the distribution of their outcome is closer to 1:1 line (Li et al., 2015). The plots show the similar results on the basis of KS and AD test results, which reveal that the LP-III distribution model is best-fitted for maximum number of gauge and discharge sites as compared to the GEV-I distribution model. Therefore, in this study, the LP-III distribution model can be considered to be more reliable for projecting the flood return periods as compared to GEV-I distribution model, which has been found well in correspondence with Pandey et al. (2018).

Flood Regionalization Analysis

The regional analysis of Q_{max} is an important tool which gives more reliable estimates of flood in a basin without or with insufficient flood data. The FI method is an important tool for regionalization of floods in a basin. It considers that the statistical distribution of floods within a homogenous region is similar. In this study, FI has been calculated as the ratios of estimated floods with different return periods to the Q_m of observed Q_{max}. The FI has been found highest at Yashwantnagar (8.48) gauge and discharge site followed by Hathini Kund (5.57) and Jateon (5.06) sites for 200-years return period based on LP-III distribution model (Table 4). Apart from this,

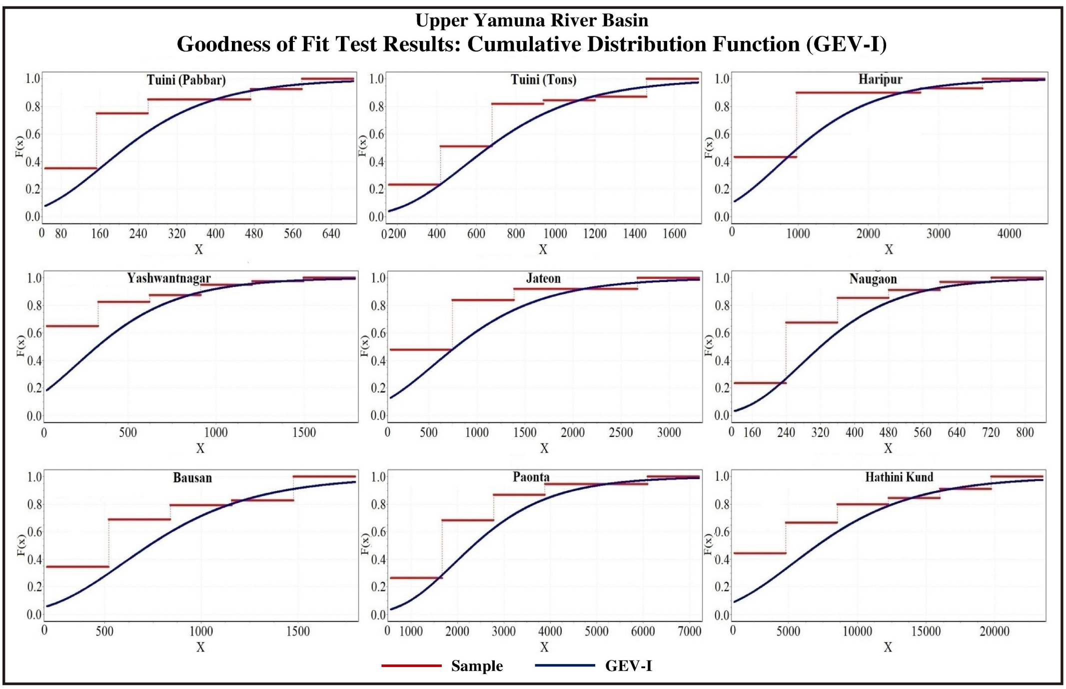

Fig. 12 (a)

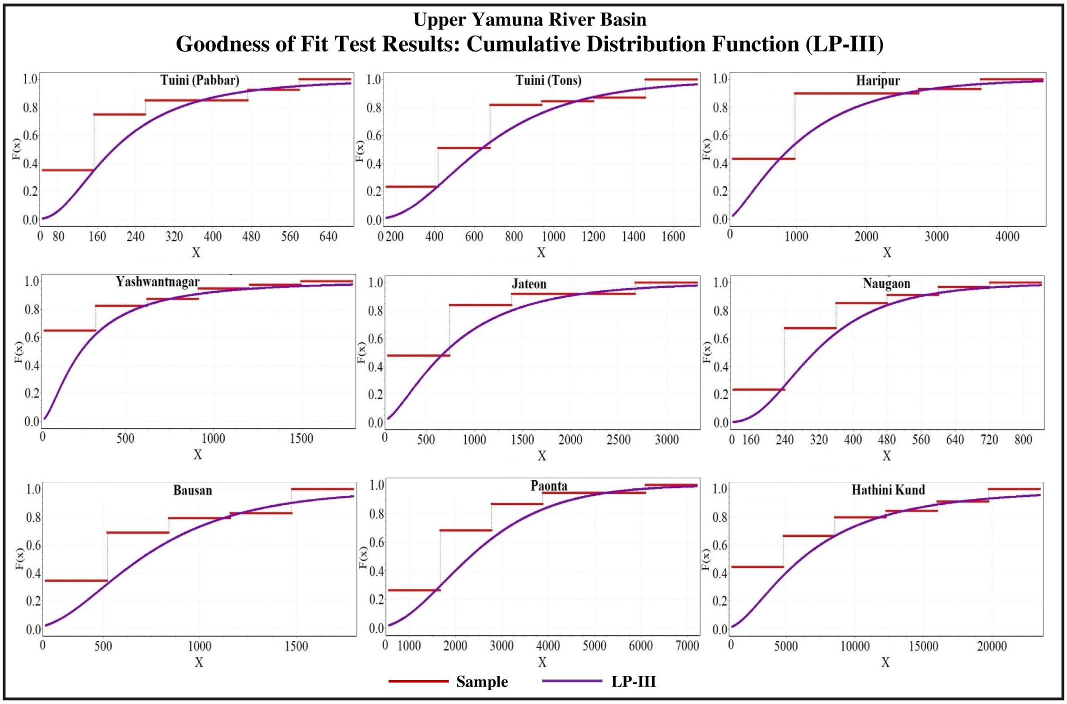

Fig. 12 (b)

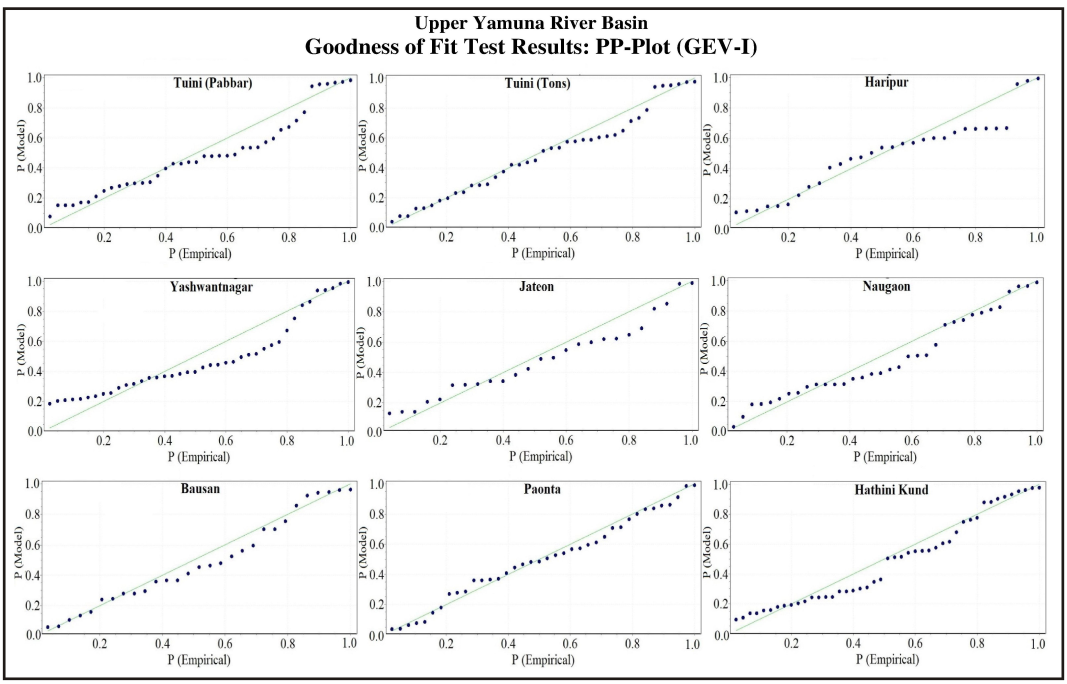

Fig. 13 (a)

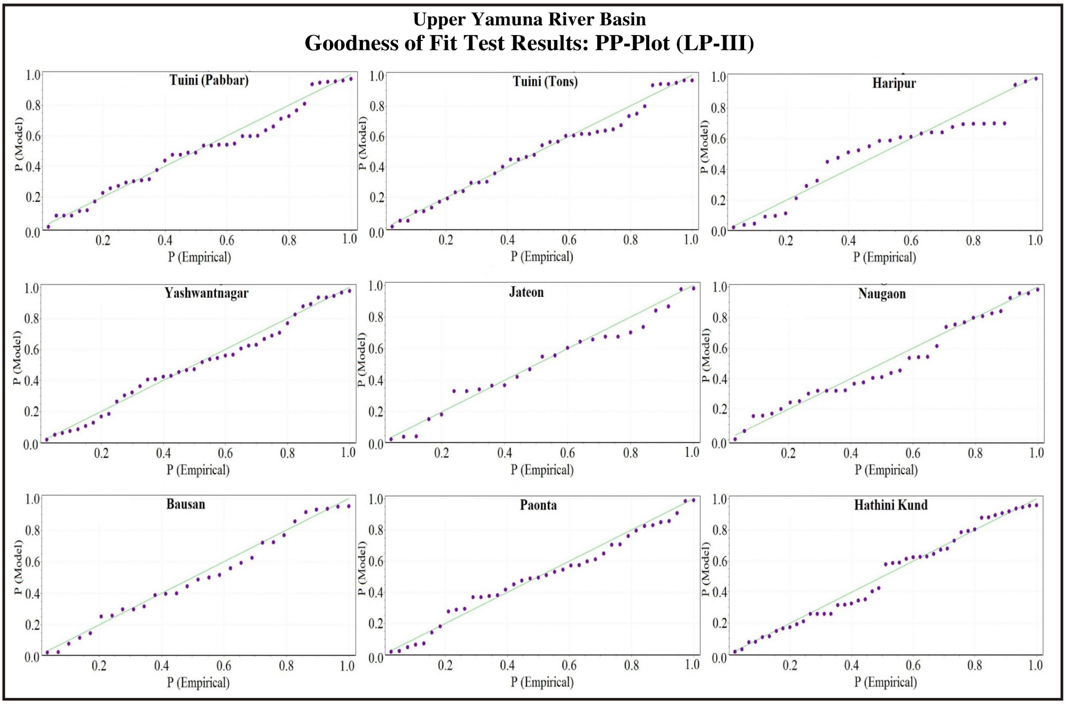

Fig. 13 (b)

flood regionalization curves have been prepared for the whole basin using both the distribution models as shown in Fig. 14. These plots reveal that on an average, the expected flood may vary between 0.8 to 4.8 times the Q_m in the upper Yamuna river basin (Fig. 14). It is important to note that the FI values differ at different gauge and discharge sites in the basin with an increase in return periods (Table 4). Pertinently, the estimated floods with higher return period are about four to five times greater than Q_m (Fig. 14).

Conclusions

This study has been carried out on the basis of annual peak flood discharge data recorded at nine gauge and discharge sites located in the upper reaches of Yamuna river. Peak flood discharges due to high intensity of south-west monsoon rainfall in the upper reaches of basin are the most severe natural disasters. Hathini Kund gauge and discharge site has recorded the largest ever peak flood discharges of 23,448, 22,837, 21,082 and 20,083 m^3/s in the years 2019, 2013, 2010 and 1978, respectively. The analysis of Q_{max} shows a high inter-annual variability in the basin as C_v varies between 47 per cent at Naugaon gauge and discharge site to 104 per cent at Yashwantnagar with a mean value of 71 per cent. The coefficient of skewness (Q_s) values for most of the gauge and discharge sites are more than 1, which indicate that at least two or more high-magnitude floods have occurred during the gauging period at these sites. The Q_{max}/Q_m ratio indicates that the largest flood recorded during the study period at each gauge and discharge site is about two to five times higher

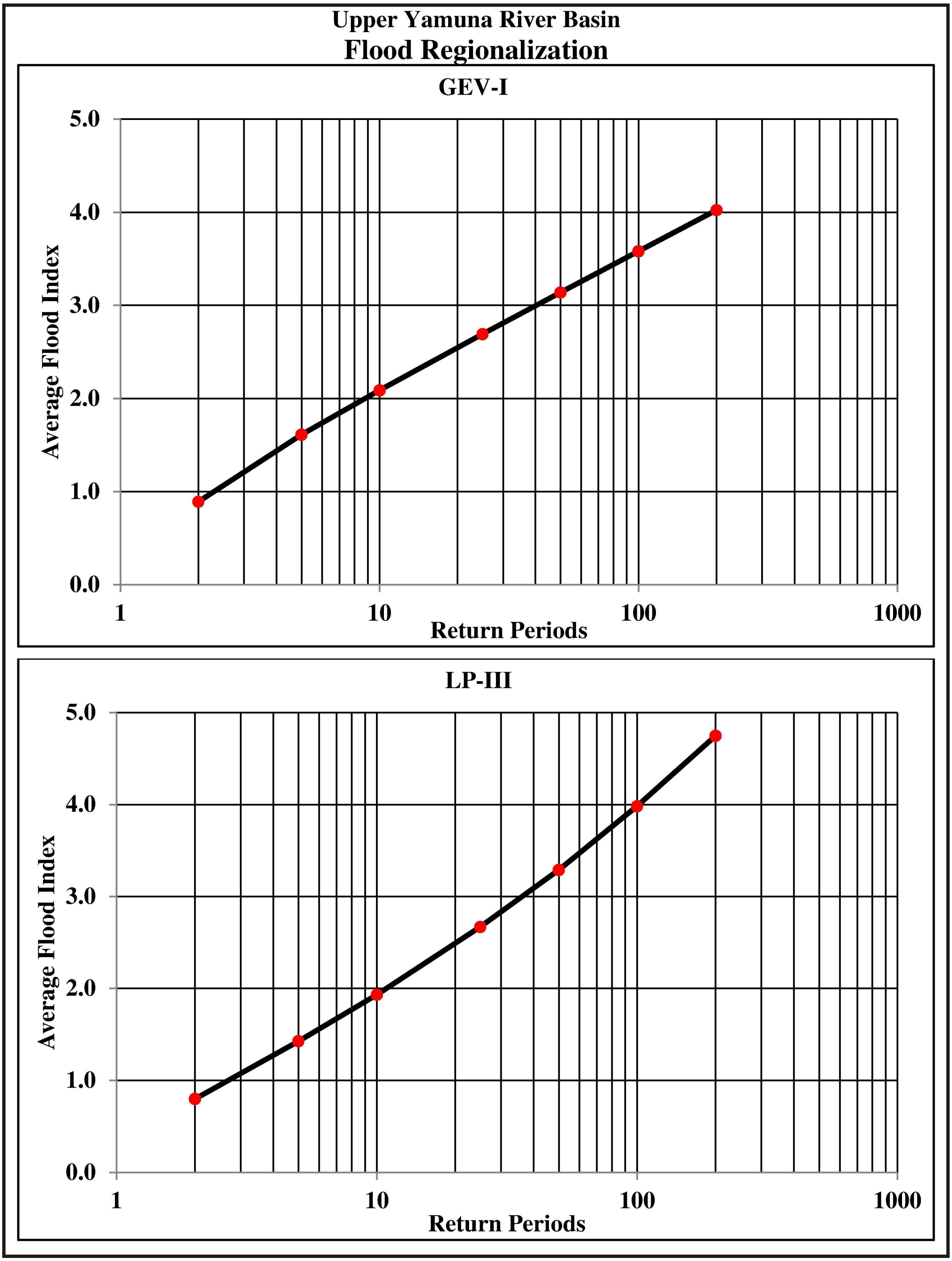
Upper Yamuna River Basin
Flood Regionalization
GEV-I
5.0
4.0
3.0
2.0
1.0
0.0
Average Flood Index
1
10
100
1000
Return Periods
LP-III
5.0
4.0
3.0
2.0
1.0
0.0
Average Flood Index
1
10
100
1000
Return Periods

Fig. 14

than the Q_m. The box plots have revealed that the Q_{max} with respect to basin area is highest at Hathini Kund gauge and discharge site with the lowest being at Tuini (Pabbar), thereby revealing that the chances of occurrence of flood are increased with the increase in basin area. The Q_{max} have shown a decreasing trend at most of the gauge and discharge sites except at Yashwantnagar, Bausan and Hathini Kund sites. Increasing Q_{max} at these sites is consistent with the hypotheses of climate change, indicating that these sites will experience more peak flood discharges in future. The plots of deviation with respect to Q_{max} from the Q_m have shown reciprocal trends as that of Q_{max} with a large inter-annual variability at all gauge and discharge sites. These results have been duly authenticated by the plots of quadratic trend model. The probability distribution used for the estimation of return periods with the magnitude of estimated discharge shows that the exceedance probability decreases with increasing time.

A comparison of the estimated discharges for 25-year return periods based on GEV-I and LP-III distribution models specifies that the estimated discharge (1700 m^3/s) calculated using the GEV-I distribution model is closer to the observed Q_{max} (1719 m^3/s) at Tuini (Tons) gauge and discharge site. Similarly, the estimated discharge for the same return periods (23,935 m^3/s) calculated using LP-III distribution model is closer to the observed Q_{max} (23,448 m^3/s) at Hathini Kund gauge and discharge site. Apart from this, a comparison of the estimated discharge for the 2-year return period has been detected below the Q_m with GEV-I and LP-III distribution models all over the basin. Similar results have been obtained for Q_{1f} with both models for 5-year return period at all gauge and discharge sites. The relationship between the Q_{max} and estimated discharges for 25-, 50-, 100- and 200-year return periods suggests that there is a positive correlation between them. The CDF and P-P plots on the basis of KS and AD test reveal that the LP-III distribution model is best-fitted for maximum number of gauge and discharge sites as compared to the GEV-I distribution model. Flood regionalization curves reveal that on an average, the expected flood may vary between 0.8 to 4.8 times the Q_m all over the basin. Finally, this study provides detailed information about the annual peak flood discharges likely to occur in the upper Yamuna river basin at nine gauge and discharge sites for the various return periods. This study, therefore, provides an input for spatial planning to reduce the risk to people, property and environment due to recurring floods in the upper basin of Yamuna river by taking appropriate measures in advance.

References

Abdul-Karim, M.D. and Chowdhury, J.U. 1995. A comparison of four distributions used in flood frequency analysis in Bangladesh. *Hydrological Sciences Journal,* 40 (1): 55-66.

Adhikari, P., Hong, Y., Douglas, K.R., Kirschbaum, D.B., Gourley, J., Adler, R. and Brakenridge, G.R. 2010. A digitized global flood inventory (1998-2008): compilation and preliminary results. *Natural Hazards,* 55 (2): 405-422.

Ang, A.H.S. and Tang, W.H. 2007. *WH Probability Concepts in Engineering: Emphasis on Applications to Civil and Environmental Engineering.* Wiley, New York: 432.

Benameur, S., Benkhaled, A., Meraghni, D., Chebana, F. and Necir, A. 2017.

Complete flood frequency analysis in Abiod watershed, Biskra (Algeria). *Natural Hazards,* 86 (2): 519-534.

Bezak, N., Brilly, M. and Sraj, M. 2014. Comparison between the peaks-over threshold method and the annual maximum method for flood frequency analysis. *Hydrological Sciences Journal,* 59 (5): 959-977.

Bhat, M.S., Ahmad, B., Alam, A., Farooq, H. and Ahmad, S. 2019a. Flood hazard assessment of the Kashmir Valley using historical hydrology. *Journal of Flood Risk Management,* 12 (S1): e12521.

Bhat, M.S., Alam, A., Ahmad, B., Kotlia, B.S., Farooq, H., Taloor, A.K. and Ahmad, S. 2019b. Flood frequency analysis of river Jhelum in Kashmir basin. *Quaternary International,* 507: 288-294.

Bobee, B., Cavidas, G., Ashkar, F., Bernier, J. and Rasmussen, P. 1993. Towards a systematic approach to comparing distributions used in flood frequency analysis. *Journal of Hydrology,* 142 (1-4): 121-136.

Bobee, B.B. and Robitaille, R. 1997. The use of the Pearson type 3 and log Pearson type 3 distributions revisited. *Water Resources Research,* 13 (2): 427-443.

Chow, V.T., Maidment, D.R. and Mays, L.W. 1988. *Applied Hydrology.* McGraw Hill Book Company, New York: 572.

Delgado, J.M., Apel, H. and Merz, B. 2010. Flood trends and variability in the Mekong river. *Hydrology and Earth System Sciences,* 14 (3): 407-418.

Ewemooje, T.A. and Ewemooje, O.S. 2011. Best distribution and plotting positions of daily maximum flood estimation at Ona river in Ogun-Oshun river basin, Nigeria. *Journal of the International Commission of Agricultural Biosystems Engineering,* 13 (3): 1-13.

Farooq, M., Shafique, M. and Khattak, M.S. 2018. Flood frequency analysis of river Swat using Log Pearson type 3, Generalized Extreme Value, Normal, and Gumbel Max distribution methods. *Arabian Journal of Geosciences,* 11: 216.

Goswami, B.N., Venugopal, V. and Sengupta, D. 2006. Increasing trend of extreme rain events over India in a warming environment. *Science,* 314 (5804): 1442-1445.

Griffis, V.W. and Stedinger, J.R. 2009. Log-Pearson type 3 distribution and its application in flood frequency analysis. III: sample skew and weighted skew estimators. *Journal of Hydrologic Engineering,* 14 (2): 121-130.

Gumbel, E.J. 1941. The return period of flood flows. *Annals of Mathematical Statistics,* 12 (2): 163-190.

Gumbel, E.J. 1958. *Statistics of Extremes.* Columbia University Press, New York: 375.

Gupta, S., Javed, A. and Datt, D. 2003. Economics of flood protection in India. *Natural Hazards,* 28 (1): 199-210.

Haktan, Y.T. 1992. Comparison of various flood frequency distributions using annual flood peaks data of rivers in Anatoli. *Journal of Hydrology,* 136 (1-4): 1-31.

Haktanir, T. 1991. Statistical modelling of maximum flows in Turkish rivers. *Hydrological Sciences Journal,* 36 (4): 367-389.

Helsel, D.R. and Hirsch, R.M. 2010. *Statistical Methods in Water Resources.* U.S. Geological Survey: 97-113.

Hire, P.S. 2000. *Geomorphic and hydrologic studies of floods in the Tapi basin.* Ph.D. dissertation, Department of Geography, University of Pune, Pune, India: 192.

Hire, P.S. and Patil, A.D. 2018. Flood frequency analysis of the Par river: Western India. *International Journal of Scientific Research in Science and Technology,* 5 (1): 164-168.

Hosking, J.R.M. and Wallis, J.R. 1993. Some statistics in regional frequency analysis. *Water Resources Research,* 29 (2): 272-281.

Ibrahim, H.M. and Isiguzo, E.A. 2009. Flood frequency analysis of Gurara river catchment at Jere, Kaduna State, Nigeria. *Scientific Research and Essays,* 4 (6): 636-646.

Ingram, W. 2016. Extreme precipitation: increases all round. *Nature Climate Change,* 6 (5): 443-444.

Izinyon, O.C., Ihimekpen, N. and Igbinoba, G.E. 2011. Flood frequency analysis of Ikpoba river catchment at Benin City using Log Pearson Type III distribution. *Journal of Emerging Trends in Engineering and Applied Sciences,* 2 (1): 50-55.

Jha, V.C. and Bairagya, H. 2011. Environmental impact of flood and their sustainable management in deltaic region of West Bengal, India. *Caminhos de Geografia,* 12 (39): 283-296.

Kale, V.S. 2003. Geomorphic effects of monsoon floods on Indian rivers. *Natural Hazards,* 28 (1): 65-84.

Kamal, V., Mukherjee, S., Singh, P., Sen, R., Vishwakarma, C.A., Sajadi, P., Asthana, H. and Rena, V. 2017. Flood frequency analysis of Ganga river at Haridwar and Garhmukteshwar. *Applied Water Science,* 7 (4): 1979-1986.

Karuna, S.S., Rajeevan, M. and Rao, S.V.B. 2016. On increasing monsoon rainstorms over India. *Natural Hazards,* 85 (3): 1743-1757.

Khattak, M.S., Anwar, F., Saeed, T.U., Sharif, M., Sheraz, K. and Ahmed, A. 2016. Floodplain mapping using HEC-RAS and Arc GIS: a case study of Kabul river. *Arabian Journal of Science and Engineering,* 41 (4): 1375-1390.

Kochel, R.C. 1988. Geomorphic impact of large floods: review and new perspectives on magnitude and frequency. In *Flood Geomorphology,* eds., Baker, V.R., Kochel, R.C. and Patton, P.C., Wiley, New York:169-187.

Koutrouvelis, I.A. and Canavos, G.C. 2000. A comparison of moment-based methods of estimation for the Log Pearson type 3 distributions. *Journal of Hydrology,* 234 (1): 71-81.

Kumar, M., Sharif, M. and Ahmad, S. 2020. Impact of urbanization on the river Yamuna basin. *International Journal of River Basin Management,* 18 (4): 461-475.

Kumar, R. 2019. Flood frequency analysis of the Rapti river basin using Log Pearson Type-III and Gumbel Extreme Value-1 methods. *Journal of the Geological Society of India,* 94 (5): 480-484.

Kumar, R., Chatterjee, C., Kumar, S., Lohani, A.K. and Singh, R.D. 2003. Development of regional flood frequency relationships using L-moments for middle Ganga plains subzone 1(f) of India. *Water Resources Management,* 17 (4): 243-257.

Latt, Z.Z. and Wittenberg, H. 2015. Hydrology and flood probability of the monsoon dominated Chindwin river in northern Myanmar. *Journal of Water and Climate Change,* 6 (1): 144-160.

Li, L., Liu, L., Guo, S. and Xiang, L. 2015. Optimal design of seasonal flood limited water levels and its application for the Three Gorges Reservoir. *Journal of Hydrology,* 527: 1045-1053.

Menon, A., Levermann, A., Schewe, J., Lehmann, J. and Frieler, K. 2013. Consistent increase in Indian monsoon rainfall and its variability across CMIP-5 models. *Earth System Dynamics,* 4 (1): 287-300.

Mishra, S.K., Gajbhiye, S. and Pandey, A. (2013). Estimation of design runoff curve numbers for Narmada watersheds (India). *Journal of Applied Water Engineering and Research,* 1 (1): 69-79.

Mohapatra, P.K. and Singh, R.D. 2003. Flood management in India. *Natural Hazards,* 28 (1): 131-143.

Onoz, B. and Bayazit, M. 1995. Best-fit distribution of largest available flood samples. *Journal of Hydrology.* 167 (1-4): 195-208.

Pandey, G.R. and Nguyen, V.T.V. 1999. A comparative study of regression-based methods in regional flood frequency analysis. *Journal of Hydrology,* 225 (1-2): 92-101.

Pandey, H.K., Dwivedi, S. and Kumar, K. 2018. Flood frequency analysis of Betwa river, Madhya Pradesh, India. *Journal of the Geological Society of India,* 92 (3): 286-290.

Patton, P.C. and Baker, V.R. 1976. Morphometry and floods in small drainage basins subject to diverse hydrogeomorphic controls. *Water Resources Research,* 12 (5): 941-952.

Pawar, U.V. and Hire, P.S. 2019. Flood frequency analysis of the Mahi Basin by using Log Pearson type III probability distribution. *Hydrospatial Analysis,* 2 (2): 102-112.

Pawar, U.V., Hire, P.S., Gunjal, R.P. and Patil, A.D. 2020. Modeling of magnitude and frequency of floods on the Narmada river, India. *Modeling Earth Systems and Environment,* 6 (4): 2505-2516.

Pearson, K. 1916. On a brief proof of the fundamental formula for testing the goodness of fit of frequency distributions and on the probable error of 'P'. *Philosophical Magazine.* 31 (6): 369-378.

Rahman, A.S., Rahman, A., Zaman, M.A., Haddad, K., Ahsan, A. and Imtiaz, M. 2013. A study on selection of probability distributions for at-site flood frequency analysis in Australia. *Natural Hazards,* 69 (3): 1803-1813.

Rao, A.R. and Hamed, H.K. 2000. *Flood Frequency Analysis.* CRC Press, Boca Raton: 376.

Rao, S.A., Dhakate, A.R., Saha, S.K., Mahapatra, S., Chaudhari, H.S., Pokhrel, S. and Sahu, S.K. 2012. Why is Indian Ocean warming consistently? *Climate Change,* 110 (3-4): 709-719.

Ray, K., Pandey, P., Pandey, C., Dimri, A.P. and Kishore, K. 2019. On the recent floods in India. *Current Science,* 117 (2): 204-218.

Renard, B., Kochanek, K., Lang, M., Garavaglia, F., Paquet, E., Neppel, L., Najib, K., Carreau, J., Arnaud, P. and Aubert, Y. 2013. Data-based comparison of frequency analysis methods: a general framework. *Water Resources Research,* 49 (2): 825-843.

Roxy, M.K., Ghosh, S., Pathak, A., Athulya, R., Mujumdar, M., Murtugudde, R., Terray, P. and Rajeevan, M. 2017. A three-fold rise in widespread extreme rain events over central India. *Nature Communications,* 8: 708.

Roxy, M.K., Ritika, K., Terray, P., Murtugudde, R., Ashok, K. and Goswami, B.N. 2015. Drying of Indian subcontinent by rapid Indian Ocean warming and a weakening land-sea thermal gradient. *Nature Communications,* 6: 7423.

Roy, P.S., Bhanumurthy, V., Murthy, C.S. and Chand, T.K. 2008. Space for disaster management: lessons and perspectives. *Journal of South Asia Disaster Studies,* 1 (1):157-177.

Sharma, D. 2012. Situation analysis of flood disaster in south and southeast Asia: A need of integrated approach. *International Journal of Science, Environment and Technology,* 1 (3): 167-173.

Shrestha, M.S. 2008. Impacts of floods in South Asia. *Journal of South Asia Disaster Studies,* 1 (1) 85-106.

Singh, O., Kasana, A., Singh, K.P. and Sarangi, A. (2020) Analysis of drivers of trends in groundwater levels under rice-wheat ecosystem in Haryana, India. *Natural Resources Research,* 29 (2):1101-1126.

Singh, O. and Kumar, M. 2013. Flood events, fatalities and damages in India from 1978 to 2006. *Natural Hazards,* 69 (3): 1815-1834.

Singh, R.B. and Singh, S. 2011. Rapid urbanization and induced flood risk in Noida, India. *Asian Geographer,* 28 (2): 147-169.

Tabari, H. 2020. Climate change impact on flood and extreme precipitation increases with water availability. *Scientific Reports,* 10: 13768.

Tanoue, M., Hirabayashi, Y. and Ikeuchi, H. 2016. Global-scale river flood vulnerability in the last 50 years. *Scientific Reports,* 6: 36021.

Trenberth, K.E., Dai, A., Rasmussen, R.M. and Parsons, D.B. 2003. The changing character of precipitation. *Bulletin of the American Meteorological Society,* 84 (9): 1205-1217.

Sachin Pandwar, Research Scholar,

Dr. Omvir Singh, Professor,
Email: osingh@kuk.ac.in
(Author for Correspondence)
Department of Geography,
Kurukshetra University,
Kurukshetra (Haryana).

punjab geographer